early phase of virus infection, e.g., at 1 dpi, but return to normal levels within a few days in a cell culture system. On the other hand, the virus-infection-induced expression of other genes, such as the extracellular signal-regulated kinase (ERK) gene, remains for a prolonged period of time (data not shown). Also, some of the gene products induced in the acute phase may suppress the expression of other genes. Under these balanced conditions, it is quite possible that certain genes are induced only at a later time, e.g., 3 to 5 dpi, but not immediately after virus infection.

It was reported previously that HCV core protein-expressing transgenic mice exhibit marked insulin resistance by inhibiting IRS-1 tyrosine phosphorylation and Akt phosphorylation (45, 58). However, our present results showed that HCV NS5A, but not the core protein, was associated with increased gluconeogenesis. Moreover, it was recently reported that HCV infection significantly inhibited cellular glucose levels at 10 dpi (69), which is quite the opposite of what we observed in the present study. These results collectively suggest the possibility that multiple pathways are involved in glucose metabolism in HCV-infected cells. Also, the possible effect(s) of the dysregulation of hepatic gluconeogenesis on the HCV life cycle needs to be clarified.

In conclusion, our present results collectively suggest that HCV promotes hepatic gluconeogenesis, resulting in increased glucose production in hepatocytes via an NS5A-mediated, FoxO1-dependent pathway.

ACKNOWLEDGMENTS

We are grateful to C. M. Rice (Rockefeller University, New York, NY) for providing Huh-7.5 cells and pFL-J6/JFH1, R. Bartenschlager (University of Heidelberg, Heidelberg, Germany) for providing an HCV subgenomic RNA replicon (pFK5B/2884Gly), and N. Kato (Okayama University, Okayama, Japan) for providing an HCV full-length RNA replicon (pON/C-5B). We also thank T. Adachi (Kyoto Prefectural University of Medicine, Kyoto, Japan), K. Igarashi, K. Kashikura, and A. Suzuki (Keio University, Yamagata, Japan) for their technical assistance.

This work was supported in part by grants-in-aid for research on hepatitis from the Ministry of Health, Labor, and Welfare, Japan, and the Japan Initiative for Global Research Network on Infectious Diseases (J-GRID) program of the Ministry of Education, Culture, Sports, Science, and Technology, Japan. This study was also carried out as part of the Global Center of Excellence program of the Kobe University Graduate School of Medicine and the Science and Technology Research Partnership for Sustainable Development (SATREPS) program of the Japan Science and Technology Agency (JST) and the Japan International Cooperation Agency (JICA).

REFERENCES

1. **Aguirre, V., T. Uchida, L. Yenush, R. Davis, and M. F. White.** 2000. The c-Jun NH(2)-terminal kinase promotes insulin resistance during association with insulin receptor substrate-1 and phosphorylation of Ser(307). J. Biol. Chem. **275:**9047–9054.
2. **Alaei, M., and F. Negro.** 2008. Hepatitis C virus and glucose and lipid metabolism. Diabetes Metab. **34:**692–700.
3. **Aytug, S., D. Reich, L. E. Sapiro, D. Bernstein, and N. Begum.** 2003. Impaired IRS-1/PI3-kinase signaling in patients with HCV: a mechanism for increased prevalence of type 2 diabetes. Hepatology **38:**1384–1392.
4. **Banerjee, A., K. Meyer, B. Mazumdar, R. B. Ray, and R. Ray.** 2010. Hepatitis C virus differentially modulates activation of forkhead transcription factors and insulin-induced metabolic gene expression. J. Virol. **84:**5936–5946.
5. **Baron, A. D., L. Schaeffer, P. Shragg, and O. G. Kolterman.** 1987. Role of hyperglucagonemia in maintenance of increased rates of hepatic glucose output in type II diabetics. Diabetes **36:**274–283.
6. **Bennett, B. L., et al.** 2001. SP600125, an anthrapyrazolone inhibitor of Jun N-terminal kinase. Proc. Natl. Acad. Sci. U. S. A. **98:**13681–13686.
7. **Blight, K. J., J. A. McKeating, and C. M. Rice.** 2002. Highly permissive cell lines for subgenomic and genomic hepatitis C virus RNA replication. J. Virol. **76:**13001–13014.
8. **Brunet, A., et al.** 2004. Stress-dependent regulation of FOXO transcription factors by the SIRT1 deacetylase. Science **303:**2011–2015.
9. **Bungyoku, Y., et al.** 2009. Efficient production of infectious hepatitis C virus with adaptive mutations in cultured hepatoma cells. J. Gen. Virol. **90:**1681–1691.
10. **Burdette, D., M. Olivarez, and G. Waris.** 2010. Activation of transcription factor Nrf2 by hepatitis C virus induces the cell-survival pathway. J. Gen. Virol. **91:**681–690.
11. **Caronia, S., et al.** 1999. Further evidence for an association between non-insulin-dependent diabetes mellitus and chronic hepatitis C virus infection. Hepatology **30:**1059–1063.
12. **Choi, J., and J. H. Ou.** 2006. Mechanisms of liver injury. III. Oxidative stress in the pathogenesis of hepatitis C virus. Am. J. Physiol. Gastrointest. Liver Physiol. **290:**G847–G851.
13. **Clore, J. N., J. Stillman, and H. Sugerman.** 2000. Glucose-6-phosphatase flux in vitro is increased in type 2 diabetes. Diabetes **49:**969–974.
14. **Deng, L., et al.** 2008. Hepatitis C virus infection induces apoptosis through a Bax-triggered, mitochondrion-mediated, caspase 3-dependent pathway. J. Virol. **82:**10375–10385.
15. **Deng, L., et al.** 2006. NS3 protein of hepatitis C virus associates with the tumour suppressor p53 and inhibits its function in an NS3 sequence-dependent manner. J. Gen. Virol. **87:**1703–1713.
16. **Diamond, D. L., et al.** 2010. Temporal proteome and lipidome profiles reveal hepatitis C virus-associated reprogramming of hepatocellular metabolism and bioenergetics. PLoS Pathog. **6:**e1000719.
17. **Dionisio, N., et al.** 2009. Hepatitis C virus NS5A and core proteins induce oxidative stress-mediated calcium signalling alterations in hepatocytes. J. Hepatol. **50:**872–882.
18. **Doi, H., C. Apichartpiyakul, K. I. Ohba, M. Mizokami, and H. Hotta.** 1996. Hepatitis C virus (HCV) subtype prevalence in Chiang Mai, Thailand, and identification of novel subtypes of HCV major type 6. J. Clin. Microbiol. **34:**569–574.
19. **Dunning, B. E., and J. E. Gerich.** 2007. The role of alpha-cell dysregulation in fasting and postprandial hyperglycemia in type 2 diabetes and therapeutic implications. Endocr. Rev. **28:**253–283.
20. **Eslam, M., M. A. Khattab, and S. A. Harrison.** 2011. Insulin resistance and hepatitis C: an evolving story. Gut **60:**1139–1151.
21. **Essers, M. A., et al.** 2004. FOXO transcription factor activation by oxidative stress mediated by the small GTPase Ral and JNK. EMBO J. **23:**4802–4812.
22. **Franck, N., J. Le Seyec, C. Guguen-Guillouzo, and L. Erdtmann.** 2005. Hepatitis C virus NS2 protein is phosphorylated by the protein kinase CK2 and targeted for degradation to the proteasome. J. Virol. **79:**2700–2708.
23. **Galossi, A., R. Guarisco, L. Bellis, and C. Puoti.** 2007. Extrahepatic manifestations of chronic HCV infection. J. Gastrointestin. Liver Dis. **16:**65–73.
24. **Gottwein, J. M., et al.** 2009. Development and characterization of hepatitis C virus genotype 1-7 cell culture systems: role of CD81 and scavenger receptor class B type I and effect of antiviral drugs. Hepatology **49:**364–377.
25. **Gross, D. N., A. P. van den Heuvel, and M. J. Birnbaum.** 2008. The role of FoxO in the regulation of metabolism. Oncogene **27:**2320–2336.
26. **Hirota, K., et al.** 2008. A combination of HNF-4 and Foxo1 is required for reciprocal transcriptional regulation of glucokinase and glucose-6-phosphatase genes in response to fasting and feeding. J. Biol. Chem. **283:**32432–32441.
27. **Hoehn, K. L., et al.** 2009. Insulin resistance is a cellular antioxidant defense mechanism. Proc. Natl. Acad. Sci. U. S. A. **106:**17787–17792.
28. **Hotamisligil, G. S.** 2005. Role of endoplasmic reticulum stress and c-Jun NH2-terminal kinase pathways in inflammation and origin of obesity and diabetes. Diabetes **54**(Suppl. 2)**:**S73–S78.
29. **Houstis, N., E. D. Rosen, and E. S. Lander.** 2006. Reactive oxygen species have a causal role in multiple forms of insulin resistance. Nature **440:**944–948.
30. **Huang, H., and D. J. Tindall.** 2007. Dynamic FoxO transcription factors. J. Cell Sci. **120:**2479–2487.
31. **Ikeda, M., et al.** 2005. Efficient replication of a full-length hepatitis C virus genome, strain O, in cell culture, and development of a luciferase reporter system. Biochem. Biophys. Res. Commun. **329:**1350–1359.
32. **Inubushi, S., et al.** 2008. Hepatitis C virus NS5A protein interacts with and negatively regulates the non-receptor protein tyrosine kinase Syk. J. Gen. Virol. **89:**1231–1242.
33. **Iynedjian, P. B., et al.** 1989. Differential expression and regulation of the glucokinase gene in liver and islets of Langerhans. Proc. Natl. Acad. Sci. U. S. A. **86:**7838–7842.
34. **Joyce, M. A., et al.** 2009. HCV induces oxidative and ER stress, and sensitizes infected cells to apoptosis in SCID/Alb-uPA mice. PLoS Pathog. **5:**e1000291.
35. **Kamata, H., et al.** 2005. Reactive oxygen species promote TNFalpha-induced death and sustained JNK activation by inhibiting MAP kinase phosphatases. Cell **120:**649–661.
36. **Karpac, J., and H. Jasper.** 2009. Insulin and JNK: optimizing metabolic homeostasis and lifespan. Trends Endocrinol. Metab. **20:**100–106.
37. **Kasai, D., et al.** 2009. HCV replication suppresses cellular glucose uptake

through down-regulation of cell surface expression of glucose transporters. J. Hepatol. **50:**883–894.
38. **Kops, G. J., and B. M. Burgering.** 1999. Forkhead transcription factors: new insights into protein kinase B (c-akt) signaling. J. Mol. Med. **77:**656–665.
39. **Lindenbach, B. D., et al.** 2005. Complete replication of hepatitis C virus in cell culture. Science **309:**623–626.
40. **Lindenbach, B. D., and C. M. Rice.** 2005. Unravelling hepatitis C virus replication from genome to function. Nature **436:**933–938.
41. **Lohmann, V., F. Korner, A. Dobierzewska, and R. Bartenschlager.** 2001. Mutations in hepatitis C virus RNAs conferring cell culture adaptation. J. Virol. **75:**1437–1449.
42. **Lowell, B. B., and G. I. Shulman.** 2005. Mitochondrial dysfunction and type 2 diabetes. Science **307:**384–387.
43. **Mehta, S. H., et al.** 2000. Prevalence of type 2 diabetes mellitus among persons with hepatitis C virus infection in the United States. Ann. Intern. Med. **133:**592–599.
44. **Mitsuyoshi, H., et al.** 2008. Evidence of oxidative stress as a cofactor in the development of insulin resistance in patients with chronic hepatitis C. Hepatol. Res. **38:**348–353.
45. **Miyamoto, H., et al.** 2007. Involvement of the PA28gamma-dependent pathway in insulin resistance induced by hepatitis C virus core protein. J. Virol. **81:**1727–1735.
46. **Morino, K., K. F. Petersen, and G. I. Shulman.** 2006. Molecular mechanisms of insulin resistance in humans and their potential links with mitochondrial dysfunction. Diabetes **55**(Suppl. 2)**:**S9–S15.
47. **Nomura-Takigawa, Y., et al.** 2006. Non-structural protein 4A of hepatitis C virus accumulates on mitochondria and renders the cells prone to undergoing mitochondria-mediated apoptosis. J. Gen. Virol. **87:**1935–1945.
48. **Ozcan, U., et al.** 2004. Endoplasmic reticulum stress links obesity, insulin action, and type 2 diabetes. Science **306:**457–461.
49. **Park, K. J., et al.** 2003. Hepatitis C virus NS5A protein modulates c-Jun N-terminal kinase through interaction with tumor necrosis factor receptor-associated factor 2. J. Biol. Chem. **278:**30711–30718.
50. **Puigserver, P., et al.** 2003. Insulin-regulated hepatic gluconeogenesis through FOXO1-PGC-1alpha interaction. Nature **423:**550–555.
51. **Reed, K. E., and C. M. Rice.** 2000. Overview of hepatitis C virus genome structure, polyprotein processing, and protein properties. Curr. Top. Microbiol. Immunol. **242:**55–84.
52. **Rozance, P. J., et al.** 2008. Chronic late-gestation hypoglycemia upregulates hepatic PEPCK associated with increased PGC1alpha mRNA and phosphorylated CREB in fetal sheep. Am. J. Physiol. Endocrinol. Metab. **294:** E365–E370.
53. **Sale, E. M., and G. J. Sale.** 2008. Protein kinase B: signalling roles and therapeutic targeting. Cell. Mol. Life Sci. **65:**113–127.
54. **Schmoll, D., et al.** 2000. Regulation of glucose-6-phosphatase gene expression by protein kinase Balpha and the forkhead transcription factor FKHR. Evidence for insulin response unit-dependent and -independent effects of insulin on promoter activity. J. Biol. Chem. **275:**36324–36333.
55. **Sekine-Osajima, Y., et al.** 2008. Development of plaque assays for hepatitis C virus-JFH1 strain and isolation of mutants with enhanced cytopathogenicity and replication capacity. Virology **371:**71–85.
56. **Seo, H. Y., et al.** 2010. Endoplasmic reticulum stress-induced activation of activating transcription factor 6 decreases cAMP-stimulated hepatic gluconeogenesis via inhibition of CREB. Endocrinology **151:**561–568.
57. **Shepard, C. W., L. Finelli, and M. J. Alter.** 2005. Global epidemiology of hepatitis C virus infection. Lancet Infect. Dis. **5:**558–567.
58. **Shintani, Y., et al.** 2004. Hepatitis C virus infection and diabetes: direct involvement of the virus in the development of insulin resistance. Gastroenterology **126:**840–848.
59. **Simmonds, P., et al.** 2005. Consensus proposals for a unified system of nomenclature of hepatitis C virus genotypes. Hepatology **42:**962–973.
60. **Soga, T., et al.** 2006. Differential metabolomics reveals ophthalmic acid as an oxidative stress biomarker indicating hepatic glutathione consumption. J. Biol. Chem. **281:**16768–16776.
61. **Soga, T., et al.** 2009. Metabolomic profiling of anionic metabolites by capillary electrophoresis mass spectrometry. Anal. Chem. **81:**6165–6174.
62. **Streeper, R. S., et al.** 1997. A multicomponent insulin response sequence mediates a strong repression of mouse glucose-6-phosphatase gene transcription by insulin. J. Biol. Chem. **272:**11698–11701.
63. **Sunayama, J., F. Tsuruta, N. Masuyama, and Y. Gotoh.** 2005. JNK antagonizes Akt-mediated survival signals by phosphorylating 14-3-3. J. Cell Biol. **170:**295–304.
64. **Takashima, M., et al.** 2010. Role of KLF15 in regulation of hepatic gluconeogenesis and metformin action. Diabetes **59:**1608–1615.
65. **Tsuruta, F., et al.** 2004. JNK promotes Bax translocation to mitochondria through phosphorylation of 14-3-3 proteins. EMBO J. **23:**1889–1899.
66. **van der Horst, A., and B. M. Burgering.** 2007. Stressing the role of FoxO proteins in lifespan and disease. Nat. Rev. Mol. Cell Biol. **8:**440–450.
67. **van der Horst, A., et al.** 2006. FOXO4 transcriptional activity is regulated by monoubiquitination and USP7/HAUSP. Nat. Cell Biol. **8:**1064–1073.
68. **Wang, A. G., et al.** 2009. Non-structural 5A protein of hepatitis C virus induces a range of liver pathology in transgenic mice. J. Pathol. **219:**253–262.
69. **Woodhouse, S. D., et al.** 2010. Transcriptome sequencing, microarray, and proteomic analyses reveal cellular and metabolic impact of hepatitis C virus infection in vitro. Hepatology **52:**443–453.
70. **Yoshida, K., T. Yamaguchi, T. Natsume, D. Kufe, and Y. Miki.** 2005. JNK phosphorylation of 14-3-3 proteins regulates nuclear targeting of c-Abl in the apoptotic response to DNA damage. Nat. Cell Biol. **7:**278–285.
71. **Zhang, S., J. Liu, G. MacGibbon, M. Dragunow, and G. J. Cooper.** 2002. Increased expression and activation of c-Jun contributes to human amylin-induced apoptosis in pancreatic islet beta-cells. J. Mol. Biol. **324:**271–285.
72. **Zhao, X., et al.** 2004. Multiple elements regulate nuclear/cytoplasmic shuttling of FOXO1: characterization of phosphorylation- and 14-3-3-dependent and -independent mechanisms. Biochem. J. **378:**839–849.

Virology 410 (2011) 38–47

Contents lists available at ScienceDirect

Virology

journal homepage: www.elsevier.com/locate/yviro

Chaperonin TRiC/CCT participates in replication of hepatitis C virus genome via interaction with the viral NS5B protein

Yasushi Inoue [a,b,c], Hideki Aizaki [a], Hiromichi Hara [a], Mami Matsuda [a], Tomomi Ando [a], Tetsu Shimoji [a], Kyoko Murakami [a], Takahiro Masaki [a], Ikuo Shoji [d], Sakae Homma [b], Yoshiharu Matsuura [e], Tatsuo Miyamura [a], Takaji Wakita [a], Tetsuro Suzuki [a,f,*]

[a] Department of Virology II, National Institute of Infectious Diseases, Tokyo 162-8640, Japan
[b] Department of Respiratory Medicine, Toho University School of Medicine, Tokyo 143-8541, Japan
[c] International University of Health and Welfare, Mita Hospital, Tokyo 108-8329, Japan
[d] Division of Microbiology, Kobe University Graduate School of Medicine, Hyogo 650-0017, Japan
[e] Research Institute for Microbial Diseases, Osaka University, Osaka 565-0871, Japan
[f] Department of Infectious Diseases, Hamamatsu University School of Medicine, Hamamatsu 431-3192, Japan

ARTICLE INFO

Article history:
Received 12 June 2010
Returned to author for revision 18 July 2010
Accepted 15 October 2010
Available online 18 November 2010

Keywords:
Hepatitis C virus
Replication
Non-structural protein
Chaperonin

ABSTRACT

To identify the host factors implicated in the regulation of hepatitis C virus (HCV) genome replication, we performed comparative proteome analyses of HCV replication complex (RC)-rich membrane fractions prepared from cells harboring genome-length bicistronic HCV RNA at the exponential and stationary growth phases. We found that the eukaryotic chaperonin T-complex polypeptide 1 (TCP1)-ring complex/chaperonin-containing TCP1 (TRiC/CCT) plays a role in the replication possibly through an interaction between subunit CCT5 and the viral RNA polymerase NS5B. siRNA-mediated knockdown of CCT5 suppressed RNA replication and production of the infectious virus. Gain-of-function activity was shown following co-transfection with whole eight TRiC/CCT subunits. HCV RNA synthesis was inhibited by an anti-CCT5 antibody in a cell-free assay. These suggest that recruitment of the chaperonin by the viral nonstructural proteins to the RC, which potentially facilitate folding of the RC component(s) into the mature active form, may be important for efficient replication of the HCV genome.

Introduction

Hepatitis C virus (HCV) is a major cause of chronic liver diseases, such as chronic hepatitis, hepatic steatosis, cirrhosis, and hepatocellular carcinoma (Hoofnagle, 2002; Manns et al., 2006; Saito et al., 1990; Seeff and Hoofnagle, 2003). HCV is an enveloped positive-strand RNA virus belonging to the *Hepacivirus* genus of the Flaviviridae family. Its genome of ~9.6 kb encodes a polyprotein precursor of ~3000 amino acids (aa) (Suzuki et al., 2007; Taguwa et al., 2008). The precursor polyprotein is post- or cotranslationally processed by both viral and host proteases into at least ten viral products. The nonstructural (NS) proteins NS3–NS5B are necessary and sufficient for autonomous HCV RNA replication. They form a membrane-associated replication complex (RC), in which NS5B is the RNA-dependent RNA polymerase (RdRp) that is responsible for copying the RNA genome of the virus during replication. The HCV RC has been detected in detergent-resistant membrane (DRM) structures, possibly in a lipid-raft structure (Aizaki et al., 2004; Shi et al., 2003). Cell-free RC replication activity has also been demonstrated in crude membrane fractions of HCV subgenomic replicon cells (Aizaki et al., 2004; Ali et al., 2002; Hara et al., 2009; Hardy et al., 2003; Yang et al., 2004); these cell-free systems provide semi-intact RdRp assays for biochemical dissection of viral replication.

In general, any process that occurs during viral replication is dependent on the host cell machinery and requires close interaction between viral and cellular proteins. Although evidence that host cell factors interact with HCV NS proteins and are involved in viral replication is accumulating (Moriishi and Matsuura, 2007), the cellular components of HCV RC and their functional roles in viral replication are not fully understood.

Recently, using comparative proteome analysis, we identified 27 cellular proteins that were highly enriched in the DRM fraction of HCV replicon cells relative to parental cells. Subsequent analyses demonstrated that one of the identified proteins, creatine kinase B, a key ATP-generating enzyme, is important for efficient replication of the HCV genome and for production of the infectious virus (Hara et al., 2009).

In this study, to extend our investigation and to increase our understanding of the precise components of HCV RC and the

* Corresponding author. Department of Infectious Diseases, Hamamatsu University School of Medicine, Hamamatsu 431-3192, Japan. Fax: +81 53 435 2337.
E-mail address: tesuzuki@hama-med.ac.jp (T. Suzuki).

0042-6822/$ – see front matter © 2010 Elsevier Inc. All rights reserved.
doi:10.1016/j.virol.2010.10.026

mechanisms of viral genome replication, we designed another comparative proteomic approach in which cells harboring genome-length bicistronic HCV RNA at the exponential growth phase (showing rapid replication of viral RNA) were compared with cells at the confluent-growth phase (showing poor replication of viral RNA). This strategy revealed that the chaperonin T-complex polypeptide (TCP1)-ring complex/chaperonin-containing TCP1 (TRiC/CCT) participates in HCV RNA replication and virion production possibly through an interaction between CCT5 (chaperonin-containing TCP1, subunit 5) and NS5B.

Results

CCT5 and Hsc70 are enriched in the DRM fraction containing the HCV RC

Recently, we analyzed the protein content of DRM fractions prepared from HCV subgenomic replicons and parental Huh-7 cells and identified 27 cellular proteins that were enriched in the DRM fraction prepared from the replicon cells (Hara et al., 2009). These were identified as factors that may be involved in the HCV RC and in viral replication. In fact, subsequent silencing of several genes coding for these proteins resulted in the inhibition of HCV RNA replication (Hara et al., 2009). However, it is likely that proteins unrelated to HCV replication are also included in the identified groups because long-term culture of the replicon cells under the selective pressure of G418 selects for a subpopulation of the parental cells and may induce changes in their protein expression profiles. Thus, to minimize interline differences in culture background, we further designed a comparative proteome analysis using a single cell line as follows.

HCV replication efficiency is dependent on the conditions of host cell growth. High cell density of the replicon culture has a reversible inhibitory effect on viral replication (Nelson and Tang, 2006; Pietschmann et al., 2001). Fig. 1A demonstrates that a high level of HCV RNA was detected in cells harboring the genome-length bicistronic HCV RNA, Con1 strain of genotype 1b (RCYM1) in the growth phase, whereas the RNA level declined sharply when the cells reached the stationary phase. We further compared the synthesis of HCV RNA in cell-free reaction mixtures containing the viral RC isolated from the RCYM1 cells at various cell densities (Fig. 1B). Replication activity was highest at the mid-log phase of cell growth (day 4 after seeding). By contrast, little or no RNA synthesis was observed under the confluent-growth cell culture (day 8), confirming the critical role of host cell growth conditions in the replication of the HCV genome.

Thus, to identify the host cell proteins required for HCV replication, we designed a two-dimensional fluorescence difference gel electrophoresis (2D-DIGE)-based comparative proteomics analysis of RC-rich DRM fractions prepared from RCYM1 cells at the mid-log and confluent-growth phases. Protein spots that reproducibly showed a greater than 1.5-fold difference in the mid-log growth- and the confluent phases were excised and digested by trypsin or lysylendopeptidase. Matrix-assisted laser desorption ionization–time-of-flight (MALDI-TOF) mass spectrometry (MS), which allows identification of the corresponding proteins in 9 cases (Table 1). Two increased spots that showed an increase in levels (their stereoscopic images are shown in Fig. 2A) were identified as CCT5 and Hsc70. CCT5, an epsilon subunit of chaperonin TRiC/CCT, is a 900-kDa toroid-shaped complex consisting of eight different subunits (Valpuesta et al., 2002; Yaffe et al., 1992). Hsc70, a member of the HSP70 family, is a 71-kDa heat shock cognate protein (Dworniczak and Mirault, 1987). Independent of the proteome analyses, DRM fractions and whole cell lysates were prepared from RCYM1 cells at two different growth phases (as above) and were analyzed by immunoblotting (Fig. 2B). Steady-state levels of CCT5 and Hsc70 were obviously higher in the DRM fraction prepared from the cells that were at the mid-log growth phase compared with those at the confluent phase. However, in the whole cell analyses, they were shown to be present at comparable levels during the two different growth phases. These results suggest that expression of CCT5 and Hsc70 is not enhanced in proliferating cells and that the enrichment of these proteins in the DRM fraction is possibly due to their post-translational modification. It should be noted that in the previous proteome analysis, CCT5 and other TRiC/CCT subunits, such as CCT1 and CCT2, were identified as proteins that were enriched in the DRM fraction prepared from subgenomic replicon-containing cells compared with that prepared from parental cells (Hara et al., 2009). We showed that CCT5 and CCT1 were enriched in the DRM fractions of cells transfected with the HCV genomic RNA derived from JFH-1 isolate as well as of subgenomic replicon cells (Fig. 2C).

TRiC/CCT participates in replication of the HCV genome

We investigated gain- and loss-of-functions of TRiC/CCT and Hsc70 with respect to the replication of HCV RNA. Seventy-two hours after RCYM1 cells were transfected with eight plasmids corresponding to each of the TRiC/CCT subunits, the level of HCV RNA in the cells (determined by quantitative RT-PCR) significantly increased to 2-fold that observed in the control cells. However, exogenous expression of Hsc70 in the RCYM1 cells showed no effect on the viral RNA (Fig. 3A). siRNAs targeted to CCT5 or Hsc70 and consisting of pools of three target-specific siRNAs or control nonspecific siRNAs were transfected

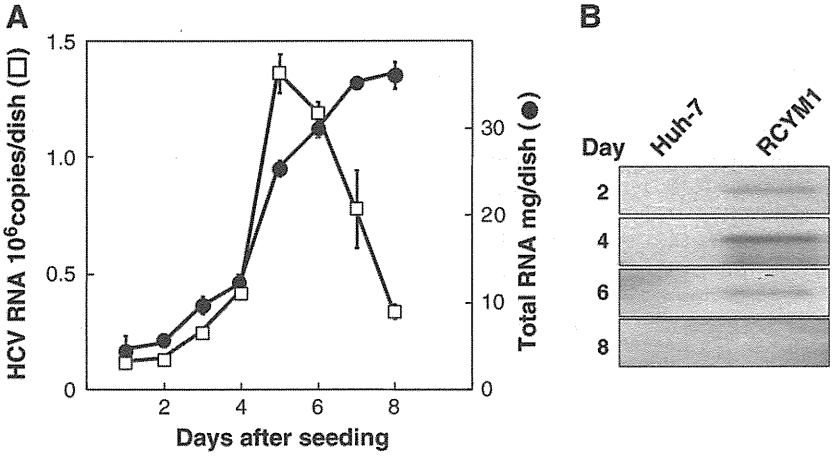

Fig. 1. Effect of cell growth on HCV RNA replication. (A) Measurement of HCV RNA (open squares) and total cellular RNA (closed circles) in RCYM1 cells at the time of harvest (days after seeding). (B) DRM fractions obtained from RCYM1 and parental Huh-7 cells harvested as indicated (day) were analyzed by cell-free RNA replication assay. RNA extracted from each sample was analyzed by agarose gel electrophoresis and autoradiograph.

Table 1
Selected cellular proteins that reproducibly increased and decreased in membrane fraction of RCYM1 cells at exponential growth phase.

Av. ratio	T-test	Coverage (%)	Protein name	Molecular function	GI
Increased proteins					
1.58	0.017	31	CCT5	Protein folding	33879913
1.54	0.005	35	HSPA8 (Hsc70)	Protein folding	24657660
Decreased proteins					
−1.95	0.028	44	Creatine kinase isozyme CK-B gene, exon 8	Energy pathway/metabolism	180568
−1.53	0.011	16	Chain C, Human Sirt2 Histone deacetylase	Cell cycle control	15826438
−2.14	0.001	33	Proteasome regulatory particle subunit p44S10	Metabolism	15341748
−1.71	0.004	21	Aldehyde dehydrogenase	Metabolism	178388
−1.85	0.004	40	Aminoacylase 1	Metabolism	12804328
−2.77	0.003	15	Eukaryotic translation initiation factor 3, subunit 3 gamma	Metabolism (translation regulator activity)	6685512
−2.43	0.014	20	Intraflagellar transport protein 74 homolog (Coiled-coil domain-containing protein 2)	Cell growth and/or maintenance	10439078

Three paired samples of RC-rich membrane fractions at the exponential- and confluent-growth phases of RCYM1 cultures were analyzed. The proteins representing a more than 1.5-fold increase or decrease (−) reproducibly and significantly are indicated.
Coverage (%): the ratio of the portion of protein sequence covered by matched peptides to the whole sequence.
GI: GenInfo Identifier number.

into RCYM1 cells. After 72 h, the HCV RNA level was reduced by 42% and 27% in the cells transfected with siRNAs against CCT5 and Hsc70, respectively, compared with controls (Fig. 3B). TRiC/CCT possibly interacts with Hsc70, and its complex formation contributes to increasing the efficiency of protein folding (Cuéllar et al., 2008). Our results suggest the involvement of TRiC/CCT and Hsc70 in the HCV life cycle. In particular, TRiC/CCT may play an important role in the replication of the viral genome.

To verify the specificity of the knockdown of CCT5 siRNA, we further synthesized two siRNAs targeted to different regions used in the above CCT5 siRNA and assessed their knockdown effect on HCV genome replication (Fig. 3C, upper panel). As expected, transfection of

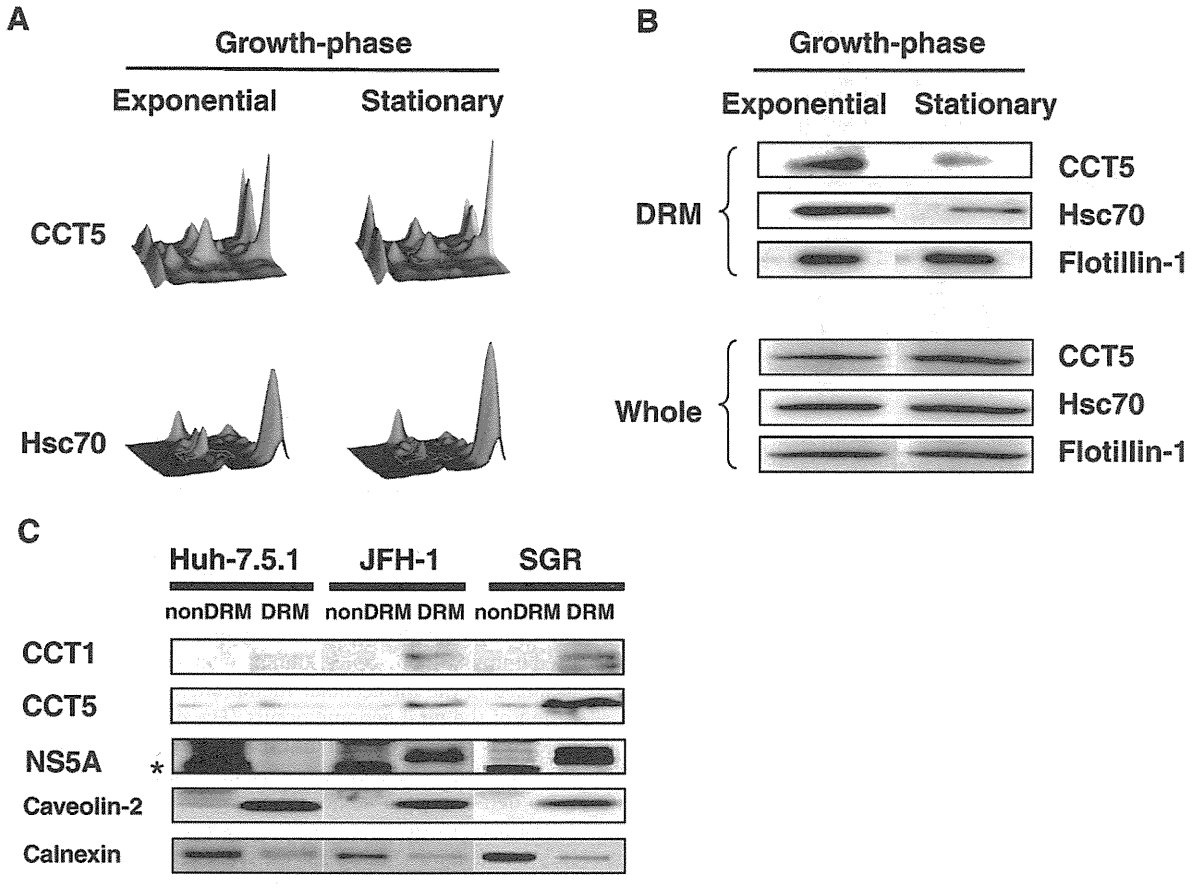

Fig. 2. Comparison of protein levels in DRM fractions prepared from RCYM1 cells at the exponential and stationary growth phases. (A) Three-dimensional images of CCT5 and Hsc70 analyzed by Ettan DIGE (GE Healthcare). Spots corresponding to CCT5/Hsc70 at exponential and stationary growth phases of the cells, respectively, are shown in green and red. (B) Equal amounts of protein in the DRM fractions prepared from RCYM1 cells at the exponential and stationary growth phases or corresponding whole cell lysates were analyzed by immunoblotting with Abs against CCT5, Hsc70 or flotillin-1. (C) Enrichment of CCT1 and CCT5 in the DRM fractions of HCV RNA replicating cells. Equal amounts of DRM or non-DRM fractions from full-length JFH-1 RNA transfected cells (JFH-1), subgenomic replicon cells (SGR) and parental Huh-7.5.1 cells were analyzed by immunoblotting with antibodies against CCT1, CCT5, NS5A, caveolin-2 or calnexin. *Non-specific bands.

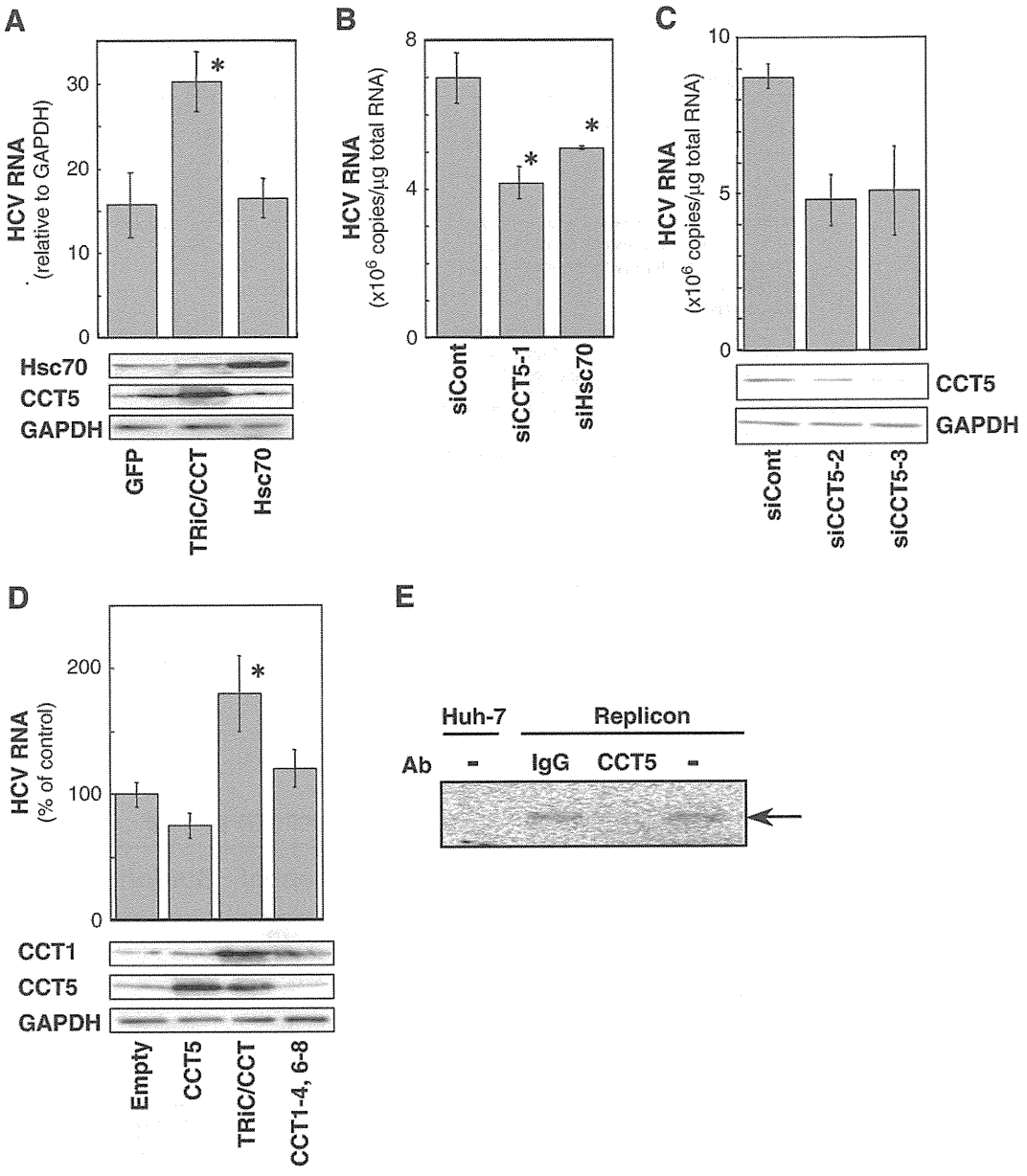

Fig. 3. Involvement of TRiC/CCT in HCV replication (A and D). Overexpression of all eight subunits of TRiC/CCT (TRiC/CCT); seven subunits, CCT1, 2, 3, 4, 6, 7, and 8 (CCT1–4, 6–8); subunit CCT5 only (CCT5); Hsc70; or control GFP in RCYM1 cells. HCV RNA levels were determined 48 h post-transfection (B and C). Knockdown of endogenous CCT5 or Hsc70 in RCYM1 cells, which were transfected with three types of siRNAs against CCT5 (siCCT5-1, -2, and -3), siRNA against Hsc70 (siHsc70), or control siRNA (siCont), and were harvested at 72 h post-transfection. siCCT5-1 and siHsc70 consisted of pools of three target-specific siRNAs. Immunoblotting for CCT1, CCT5, Hsc70 and GAPDH was performed (A, C and D; lower). (E) Cell-free de novo viral RNA synthesis assays were performed in the presence of anti-CCT5 Ab or control mouse IgG. Cytoplasmic fractions from SGR-N (replicon) and parental Huh-7 cells were used. An arrow indicates the synthesized HCV RNA. Error bars denote standard deviations with asterisks indicating statistical significance (*$P<0.01$).

RCYM1 cells with each CCT5 siRNA resulted in a reduction in viral RNA to a level of about 50% of that observed in cells treated with control siRNAs. Immunoblotting confirmed the efficient reduction in expression of endogenous CCT5 and the lack of cytotoxic effect exerted by the CCT5 siRNAs (Fig. 3C, middle and lower panels).

Having confirmed the upregulation of HCV RNA by ectopic expression of all the TRiC/CCT subunits, we further addressed the possibility that CCT5, independent of the complete TRiC/CCT complex, might have a role in promoting replication of HCV RNA. Transfection with either a CCT5 expression plasmid alone or with seven plasmids expressing all the TRiC/CCT subunits except CCT5 resulted in no or only a slight increase in the level of HCV RNA, indicating that all CCT subunits are required for HCV replication (Fig. 3D).

TRiC/CCT is generally known as a cytosolic chaperone (Valpuesta et al., 2002). However, it is enriched in the DRM fraction of HCV-replicating cells during the exponential growth phase (Fig. 2B). We used immunofluorescence staining to investigate whether TRiC/CCT is localized in the intracellular membrane compartments where replication of the viral genome occurs (Fig. 4). The de novo-synthesized RdRp was labeled by bromouridine triphosphate (BrUTP) incorporation in the presence of actinomycin D, and brominated nucleotides were detected with a specific antibody (Ab). Fluorescence staining in distinct speckles of various sizes was found in the cytoplasm of the HCV subgenomic replicon cells, whereas no signal was detected in the control cells, indicating that the observed BrUTP-incorporating RNA is mostly viral, newly synthesized viral RNA (Fig. 4A). Double immunofluorescence staining showed that a certain section of CCT5 co-distributed with the BrUTP-labeled RNA (Fig. 4A), which is known to co-exist with HCV NS proteins in viral replicating cells (Shi et al., 2003). We further observed that CCT5 was at least partially colocalized

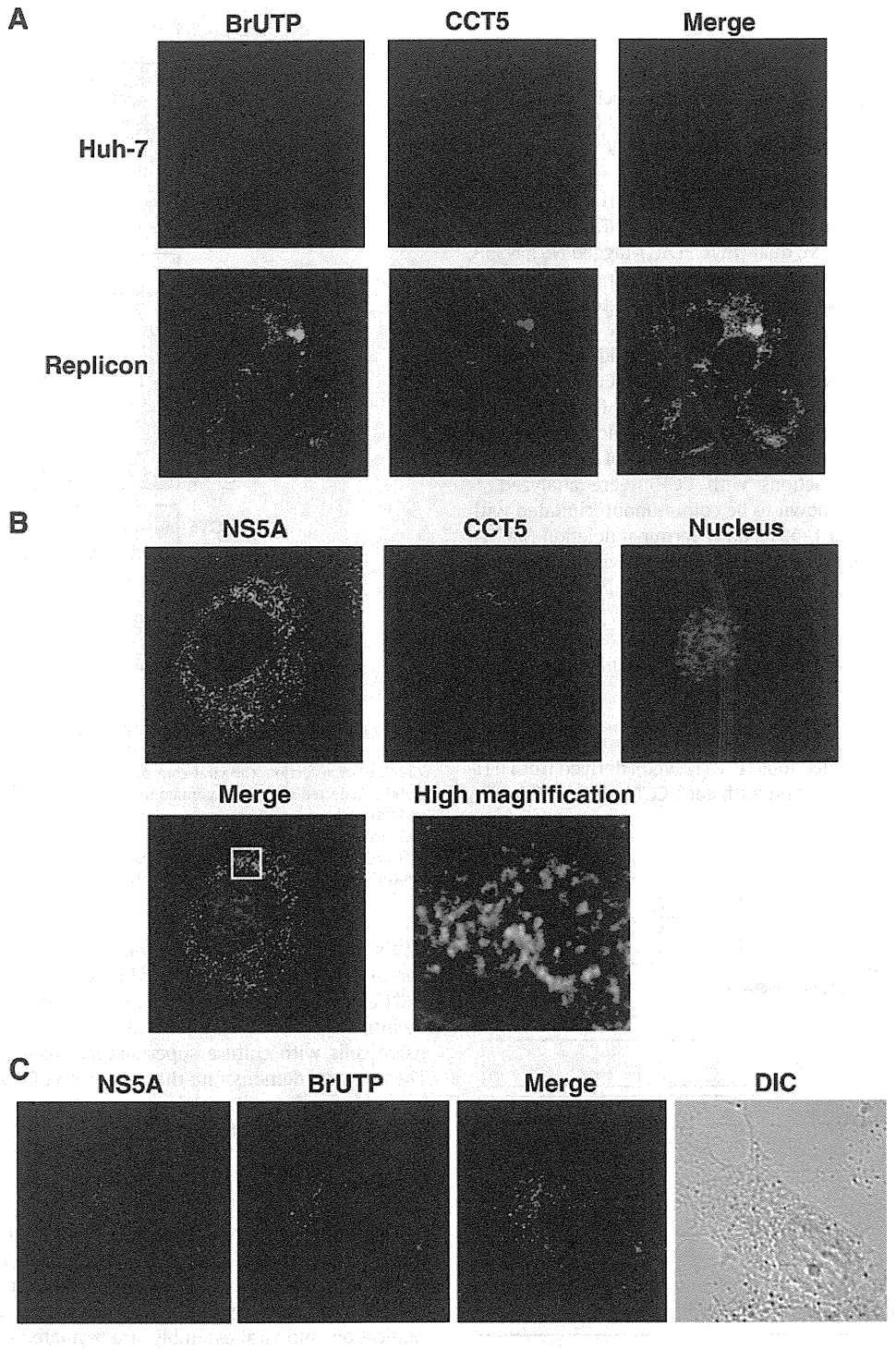

Fig. 4. Immunofluorescence analysis of CCT5 in SGR-N and Huh-7 cells (A) and HCVcc-infected cells (B). The primary Abs used were anti-CCT5 goat polyclonal Ab (red), anti-BrUTP monoclonal Ab (green), and anti-NS5A monoclonal Ab (green). Merged images of red and green signals (A) or of red, green and blue (nucleus) signals (B) are shown. The high magnification panel is an enlarged image of a white square of the merge panel. (C) Colocalization of NS5A protein with the viral RNA. The replicon cells were permeabilized with lysolecithin and labeled with BrUTP, followed by staining with anti-NS5A rabbit polyclonal Ab (red) and the anti-BrUTP monoclonal Ab (green). DIC, differential interference contrast.

with the viral NS protein in certain compartments sharing a dot-like structure in Huh-7 cells infected with HCV JFH-1 infectious HCV (HCVcc) derived from HCV genotype 2a (Fig. 4B) as well as in the replicon cells (data not shown). Fig. 4C indicated co-localization of BrUTP-labeled RNA with NS5A.

To further address the role of TRiC/CCT in HCV genome replication, we performed immunodepletion and in vitro replication analyses, which have been used for studying the genome replication of several viruses (Daikoku et al., 2006; Garcin et al., 1993; Liu et al., 2009). Cell extracts prepared from the HCV-replicating cells were reacted with either a mouse monoclonal Ab against CCT5 or mouse IgG derived from preimmune serum, followed by cell-free synthesis of HCV RNA. Fig. 3E shows that treatment with anti-CCT5 Ab inhibited viral RNA synthesis, whereas the control IgG did not affect the process, suggesting that TRiC/CCT participates directly in HCV RNA replication.

CCT5 interacts with HCV NS5B

The genome replication machinery of HCV is a membrane-associated complex composed of multiple factors including viral NS proteins. Given the involvement of TRiC/CCT in HCV RNA synthesis, we next examined its possible interaction with HCV NS proteins. A first attempt to immunoprecipitate the viral proteins with antibodies against TRiC/CCT subunits in the replicon cells was unsuccessful (data not shown), suggesting that endogenous levels of TRiC/CCT is not sufficient to pull out NS5B. Next, dual (myc/FLAG)-tagged NS3, NS5A, or NS5B proteins derived from the genotype 1b NIHJ1 strain were co-expressed with CCT5 in Huh-7 cells and then subjected to two-step immunoprecipitation with anti-myc and anti-FLAG Abs (Ichimura et al., 2005; Shirakura et al., 2007). An empty plasmid was used as a negative control in the analyses. As shown in Fig. 5A, CCT5 specifically interacted with NS5B. Little or no interaction was found between CCT5 and NS3 or NS5A. To determine the NS5B region required for the interaction with CCT5, various deletion mutants of HA-NS5B were constructed and their interactions with CCT5 were analyzed as described above. CCT5 was shown to be coimmunoprecipitated with either a full-length NS5B (aa 1–591), an N-terminal deletion (aa 71–591) or a C-terminal deletion (aa 1–570), but not with deletions aa 215–591 or aa 320–591 (Fig. 5B), suggesting that aa 71–214 of NS5B are important for its interaction with CCT5.

Knockdown of CCT5 results in the reduction of propagation of infectious HCV

We further examined whether the knockdown of CCT5 would abrogate the production of infectious HCV (HCVcc), derived from JFH-1 (Fig. 6). At 72 h post-transfection with each CCT5 siRNA, HCV RNA

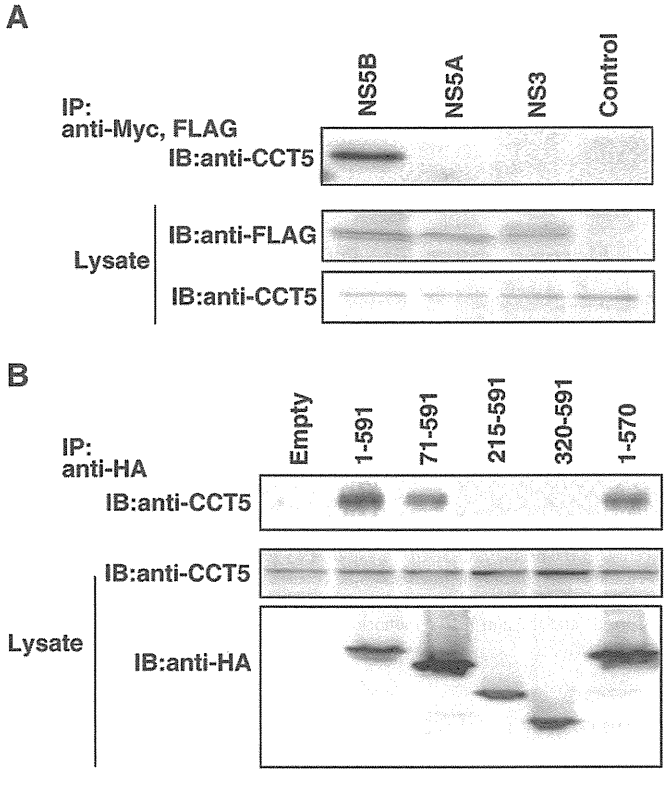

Fig. 5. CCT5 interacts with HCV NS5B. (A) CCT5 was co-expressed with MEF-tagged-NS5B, -NS5A, or -NS3 protein of strain NIHJ1 in cells, followed by two-step immunoprecipitation (IP) with anti-FLAG and anti-myc Abs. Immunoprecipitates were subjected to immunoblotting with anti-CCT5 Ab (IB). (B) Full-length NS5B (1–591) or its deletions (71–591, 215–591, 320–591, 1–570) along with a HA tag were co-expressed with CCT5. IP and IB were performed as described above.

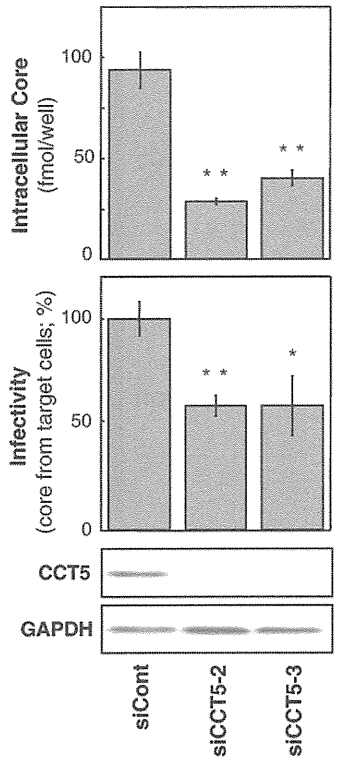

Fig. 6. Knockdown of endogenous CCT5 in HCVcc-infected cells. The cells were transfected with siRNAs against CCT5 (siCCT5-2, -3) or with control siRNAs (siCont). At 72 h post-transfection, the viral core protein levels in cells were determined (upper panel). Collected culture supernatants were inoculated into naïve Huh7.5.1 cells and intracellular core proteins were determined at 72 h post-infection (middle panel). Cells transfected with siRNAs were analyzed by immunoblotting with anti-CCT5 or anti-GAPDH Ab (lower panel). Error bars denote standard deviations with asterisks indicating statistical significance (*$P<0.05$; **$P<0.01$).

levels in Huh-7 cells infected with HCVcc were reduced by 25–35% compared with controls. Accordingly, virion production from CCT5 siRNA-transfected cultures was significantly decreased, as determined by intracellular HCV core protein levels at 72 h after the infection of naïve cells with culture supernatants taken from transfected cells. These results demonstrate that reduction of the HCV RNA replication by siRNA-mediated knockdown of CCT5 results in reduction of the propagation of the infectious virus.

Discussion

The chaperone-assisted protein-folding pathway is a process in living cells that results from coordinated interactions between multiple proteins that often form multi-component complexes. Several steps in the viral life cycle, such as protein processing, genome replication, and viral assembly, are regulated by cellular chaperones. Hsp90, one of the most abundant proteins in unstressed cells, has been implicated in HCV RNA replication (Nakagawa et al., 2007; Okamoto et al., 2006, 2008; Taguwa et al., 2008, 2009; Ujino et al., 2009). FKBP8, a member of the FKBP506-binding protein family, and hB-ind1, human butyrate-induced transcript 1, play key roles through their interaction with HCV NS5A and Hsp90 (Okamoto et al., 2006, 2008; Taguwa et al., 2008, 2009). Hsp90 has also been implicated in viral enzymatic activities including those of the influenza virus (Momose et al., 2002; Naito et al., 2007), herpes simplex virus (Burch and Weller, 2005), Flock house virus (Kampmueller and Miller, 2005), and hepatitis B virus (Hu et al., 2004).

In our former study, comparative proteome analyses of the viral RC-rich DRM fractions prepared from subgenomic replicon cells and Huh-7 cells were carried out to identify host factors involved

in HCV replication (Hara et al., 2009). We extended the proteomics by modifying our protocol of the analysis to reduce the interline differences in culture background and analyzed the DRM samples derived from the mid-log and confluent-growth phases of single cell line. Here, we identified two proteins, CCT5 and Hsc70, showing an increase in levels at the mid-log growth phase. Although CCT5 was also identified in the former study as expected, Hsc70 was not included in the list of proteins identified in the study (Hara et al., 2009). This difference may be due to the use of cells carrying the full-length replicon RNA in this study.

In this study, we demonstrated that TRiC/CCT participates in HCV RNA replication and virion production possibly through its interaction with NS5B. TRiC/CCT is a group II chaperonin that assists in protein folding in eukaryotic cells and forms a double-ring-like hexadecamer complex. Although relatively little is known about its function compared with that of the group I chaperonins such as bacterial GroEL, several mammalian proteins whose folding is mediated by TRiC/CCT have been identified, such as actin, tubulin, and von Hippel–Lindau tumor suppressor protein (Farr et al., 1997; Feldman et al., 2003; Frydman and Hartl, 1996; Meyer et al., 2003; Tian et al., 1995). With regard to viral proteins, the Epstein–Barr virus nuclear antigen, HBV capsid protein, and p4 of M-PMV have been identified as TRiC/CCT-interacting proteins (Yam et al., 2008). However, the functional significance of their interactions in the viral life cycles has yet to be determined. Here we demonstrated that the reduction in CCT5 expression in HCV replicon cells and in virus-infected cells inhibits HCV RNA replication (Figs. 3B and C) and virus production (Fig. 6) respectively. Gain-of-function was also shown by co-transfection of the replicon cells with eight constructs corresponding to all the TRiC/CCT subunits (Figs. 3A and D).

A recent study of the three-dimensional structure of the TRiC/CCT and Hsc70 complex has demonstrated that the apical domain of the CCT2 (CCT-beta) subunit is involved in the interaction with Hsc70 (Cuéllar et al., 2008). The complex formation created by the TRiC/CCT and Hsc70 interaction may promote higher efficiency in the folding of certain proteins (Cuéllar et al., 2008). In our comparative proteome analyses, both CCT subunits and Hsc70 were enriched in the HCV RC-rich membrane fraction of the replicon cells that showed high viral replication activity (Fig. 2B). Transfection of Hsc70 siRNA into the replicon cells moderately inhibited viral RNA replication (Fig. 3B). However, upregulation of HCV replication was not observed by ectopic expression of Hsc70 (Fig. 3A), and little or no interaction was observed between Hsc70 and HCV NS proteins in the co-immunoprecipitation analysis (data not shown). Thus, it is likely that TRiC/CCT acts as a regulator of HCV replication through participating in the de novo folding of NS5B RdRp, and Hsc70 might serve to assist in folding through its interaction with TRiC/CCT. It was recently reported that Hsc70 is associated with HCV particles and modulates the viral infectivity (Parent et al., 2009). Here we showed an additional role of Hsc70 in the HCV life cycle.

HCV genomic single-stranded RNA serves as a template for the synthesis of the full-length minus strand that is used for the overproduction of the virus-specific genomic RNA. NS5B RdRp is a single subunit catalytic component of the viral replication machinery responsible for both of these processes. It is known that the in vitro RdRp activity of recombinant NS5B expressed in and purified from insect cells and *Escherichia coli* is low in many cases. This could be due to the lack of a suitable cellular environment for favorable RdRp activity, although the particular conformational features dependent on the viral isolates may also be involved (Lohmann et al., 1997; Weng et al., 2009). In fact, besides interacting with HCV NS proteins, NS5B has been reported to interact with several host cell proteins. For example, human vesicle-associated membrane protein-associated protein subtype A (VAP-A) and subtype B (VAP-B), which are involved in the regulation of membrane trafficking, lipid transport and metabolism, and the unfolded protein response, interact with NS5B and NS5A and participate in HCV replication (Hamamoto et al., 2005). Recently, VAP-C, a splicing variant of VAP-B, was found to act as a negative regulator of viral replication through its interaction with NS5B but not with VAP-A (Kukihara et al., 2009). Cyclophilin A and B, peptidyl-prolyl isomerases that facilitate protein folding by catalyzing the *cis–trans* interconversion of peptide bonds at proline residues, play a role in stimulating HCV RNA synthesis through interaction with NS5B (Liu et al., 2009; Watashi et al., 2005). SNARE-like protein (Tu et al., 1999), eIF4AII (Kyono et al., 2002), protein kinase C-related kinase 2 (Kim et al., 2004), nucleolin (Kim et al., 2004; Hirano et al., 2003; Shimakami et al., 2006), and p68 (Goh et al., 2004) are also known to associate with NS5B and are possibly involved in HCV RNA replication.

We found that the aa 71–214 region in NS5B is important for interaction with TRiC/CCT. The catalytic domain of HCV RdRp has a "right-hand" configuration similar to other viral polymerases, such as HIV-1 reverse transcriptase (Huang et al., 1998) and poliovirus RdRp (Hansen et al., 1997), and is divided into the fingers, palm, and thumb functional subdomains (Lohmann et al., 2000). The region required for the interaction with TRiC/CCT has been mapped in a part of the fingers and palm domains of NS5B RdRp. To address how TRiC/CCT assists in the correct folding or disaggregation of NS5B through their interaction, leading to the formation of a functional RdRp, work based on an in vitro reconstitution system using purified proteins is under way. As all the TRiC/CCT subunits possess essentially identical ATPase domains, their protein-recognition regions are apparently divergent, allowing for substrate-binding specificity. It has recently been reported that TRiC/CCT interacts with the PB2 subunit of the influenza virus RNA polymerase complex and TRiC/CCT binding site is located in the central region of PB2, suggesting involvement of TRiC/CCT in the influenza virus life cycle (Fislová et al., 2010). Eukaryotic RNA polymerase subunit has also been identified as a binding partner of TRiC/CCT from interactome analysis (Yam et al., 2008). It would be interesting to examine how conserved the mechanisms of TRiC/CCT action that result in enhanced replication are among RNA polymerases.

The recruitment of a chaperonin by viral NS proteins may be important for understanding regulation of the viral genome replication. In this study, we demonstrated the involvement of TRiC/CCT in HCV RNA replication possibly through its interaction between TRiC/CCT and HCV NS5B. Although possible interaction of subunit CCT5 with NS5B was shown, considering involvement of whole TRiC/CCT complex in its chaperonin function, whether CCT5 directly interacts with NS5B is unclear. Further detailed studies are needed to make clear the manner of TRiC/CCT-NS5B interaction. NS5B RdRp is one of the main targets for HCV drug discovery. The search for NS5B inhibitors has resulted in the identification of several binding sites on NS5B, such as the domain adjacent to the active site and the allosteric GTP site (De Francesco and Migliaccio, 2005; Laporte et al., 2008). The findings obtained here suggest that disturbing the interaction between NS5B and TRiC/CCT may be a novel approach for an antiviral chemotherapeutic strategy.

Materials and methods

Cell culture, transfection, and infection

Human hepatoma Huh-7 and Huh-7.5.1 cells (kindly provided by Francis V. Chisari from The Scripps Research Institute) and human embryonic kidney 293T cells were maintained in Dulbecco's modified Eagle's medium (DMEM) supplemented with 10% fetal calf serum. Huh-7-derived SGR-N (Shi et al., 2003) and RCYM1 (Murakami et al., 2006) cells, which possess subgenomic replicon RNA from the HCV-N strain (Guo et al., 2001; Ikeda et al., 2002) and genome-length HCV RNA from the Con 1 strain (Pietschmann et al., 2002), were cultured in the above medium in the presence of 1 mg/ml G418. Cells were transfected with plasmid DNAs using FuGENE transfection reagents

(Roche Diagnostics, Tokyo, Japan). Culture media from Huh-7 cells transfected with in vitro-transcribed RNA corresponding to the full-length HCV RNA derived from the JFH-1 strain (Wakita et al., 2005) were collected, concentrated, and used for the infection assay (Aizaki et al., 2008).

Ab

Primary Abs used in this study were mouse monoclonal Abs against FLAG (Sigma-Aldrich, St. Louis, MO), c-myc (Sigma-Aldrich), CCT5 (Abnova Corporation, Taipei City, Taiwan), flotillin-1 (BD Biosciences, San Jose, CA), glyceraldehyde-3-phosphate dehydrogenase (GAPDH) (Chemicon, Temecula, CA), BrdU (Caltag, CA) and HCV NS5A (Austral Biologicals, San Ramon, CA), a rabbit polyclonal Ab against hemagglutinin (HA; Sigma-Aldrich), a sheep polyclonal Ab against bromodeoxyuridine (Biodesign International, Saco, ME), and goat polyclonal Abs against the individual subunits of CCT (Santa Cruz Biotechnology, Santa Cruz, CA) and Hsc70 (Santa Cruz Biotechnology). Anti Hsc70 and CCT5 monoclonal rat Abs were obtained from Abcam (Tokyo, Japan) and AbD serotec (Oxford, UK). Rabbit polyclonal antibody to NS5A was described previously (Hamamoto et al., 2005). Anti NS5B monoclonal Ab was kindly provided by D. Moradpour (Centre Hospitalier Universitaire Vaudois, University of Lausanne; Moradpour et al., 2002).

Plasmids

To generate expression plasmids for the NS proteins with dual epitope tags, DNA fragments encoding the NS3, NS5A, or NS5B proteins were amplified from HCV strain NIHJ1 (Aizaki et al., 1998) by PCR and cloned into the EcoRI–EcoRV sites of pcDNA3-MEF, which includes the MEF tag cassette containing the *myc* tag, TEV protease cleavage site, and FLAG tag sequences (Ichimura et al., 2005; Shirakura et al., 2007). To create a series of NS5B truncation mutants, each fragment was amplified by PCR and cloned into the EcoRI–XhoI site of pCMV-HA (Clontech, Mountain View, CA). To generate expression plasmids for the individual CCT subunits, cDNA fragments encoding human CCT1 through CCT8 were amplified from the total cellular RNA by RT-PCR and then cloned into the SmaI site of pCAGGS (Niwa et al., 1991). All PCR products were confirmed by nucleotide sequencing.

Proteome analysis

RC-rich membrane fractions from the cells were isolated as described previously (Aizaki et al., 2004). Briefly, cells were lysed in hypotonic buffer. After removing the nuclei, the supernatants were mixed with 70% sucrose, overlaid with 55% and 10% sucrose, and centrifuged at 38,000 rpm for 14 h. Proteins from the membrane fractions were then analyzed by 2D-DIGE as described previously (Hara et al., 2009). Briefly, protein samples were resolved in protein solubilization buffer (Bio-Rad Laboratories, Tokyo, Japan) and washed with pH adjustment buffer (7 M urea, 2 M thiourea, 4% CHAPS, 30 mM Tris–HCl [pH 10.0]), before being labeled with fluorescent dyes; the dyes used were Cy3 for RCYM1 cells samples taken at the exponential growth phase, Cy5 for cells samples taken at the confluent phase, and Cy2 for a protein standard containing equal amounts of both cell samples. Aliquots of the labeled samples were pooled and applied to Immobiline DryStrip (GE Healthcare, Tokyo, Japan) for first-dimension separation and to 12.5% polyacrylamide gels for second-dimension separation. Images of the 2-D gels were captured on a Typhoon scanner (GE Healthcare), and analyzed quantitatively using DeCyder v5.0 software (GE Healthcare). Samples were analyzed in triplicate as independent cultures and the Student's *t*-test was applied using the DeCyder biological variation analysis module to validate the significance of the differences in spot intensity detected between the samples.

In vitro RNA replication assay

In vitro replication of HCV RNA was performed as described previously (Hamamoto et al., 2005). Briefly, cytoplasmic fractions of subgenomic replicon cells were treated with 1% NP-40 at 4 °C for 1 h, followed by being incubated with 1 mM of ATP, GTP, and UTP; 10 μM CTP; [^{32}P]CTP (1 MBq; 15 TBq/mmol); 10 μg/ml actinomycin D; and 800 U/ml RNase inhibitor (Promega, Madison, WI) for 4 h at 30 °C. RNA was extracted from the total mixture by using TRI Reagent (Molecular Research Center, Cincinnati, OH). The RNA was precipitated, eluted in 10 μl of RNase-free water, and analyzed by 1% formaldehyde-agarose gel electrophoresis. For the immunodepletion assay, the cytoplasmic fractions were incubated with anti-CCT5 Ab in the presence of NP-40 for 4 h before NTP incorporation.

MALDI-TOF MS analysis

Target spots were cut and collected from gels under UV luminescence and rechecked with Typhoon scanner. The spot gels of the target proteins were subjected to in-gel trypsin digestion and analyzed by MALDI-TOF MS meter (Voyager-DE STR, Applied Biosystems, Tokyo, Japan) as described previously (Yanagida et al., 2000). All proteins were identified by peptide mass fingerprinting.

Immunoblot analysis and immunoprecipitation

Immunoblot analysis was performed essentially as described previously (Aizaki et al., 2004). The membrane was visualized with SuperSignal West Pico chemiluminescent substrate (Pierce, Rockford, IL). For immunoprecipitation, cells transfected with plasmids expressing epitope-tagged HCV protein or CCT5 were lysed and then subjected to two-step precipitations with anti-myc and anti-FLAG Abs according to the procedures described previously (Ichimura et al., 2005). In some experiments, HA-tagged full-length NS5B (aa 1–591) or its deletion mutants (aa 71–591, 215–591, 320–591, 1–570) were co-expressed with CCT5 in cells, followed by single-step immunoprecipitation and immunoblotting.

Immunofluorescence staining

Cell permeabilization with lysolecithin and detection of de novo-synthesized viral RNA was performed as described previously (Shi et al., 2003). Briefly, Huh-7 cells were plated on 8-well chamber slides at a density of 5×10^4 cells per well. Cells were incubated with actinomycin D (5 μg/μl) for 1 h and were washed twice with serum-free medium, before being incubated for 10 min on ice. The cells were then incubated in a transcription buffer containing 0.5 mM BrUTP for 30 min. The cells were fixed in 4% formaldehyde for 20 min and then incubated for 15 min in 0.1% Triton X-100 in phosphate-buffered saline (PBS). Primary Abs were diluted in 5% bovine serum albumin in PBS and were incubated with the cells for 1 h. After washing with PBS, fluorescein-conjugated secondary Abs (Jackson Immunoresearch Laboratories, West Grove, PA) were added to the cells at a 1:200 dilution for 1 h. The slides were then washed with PBS and mounted in ProLong Antifade (Molecular Probes, Eugene, OR). Confocal microscopy was performed on a Zeiss Confocal Laser Scanning Microscope LSM 510 (Carl Zeiss MicroImaging, Thornwood, NY).

RNA interference

Small interfering RNAs (siRNAs) targeted to CCT5 or Hsc70 and scrambled negative control siRNAs were purchased from Sigma-Aldrich Japan (Tokyo, Japan). Cells were plated on a 24-well plate with

antibiotic-free DMEM overnight, and each plate was transfected with 10 nM siRNAs by X-tremeGENE (Roche Diagnostics) according to the manufacturer's protocol. Forty-eight hours post-transfection, the total RNA and protein extracts were prepared and subjected to real-time RT-PCR and immunoblot analyses, respectively.

Quantitation of HCV RNA and core protein

Total RNA was extracted from cells using TRIzol reagent (Invitrogen, Carlsbad, CA) according to the manufacturer's instructions. Real-time RT-PCR was performed using TaqMan EZ RT-PCR Core Reagents (PE Applied Biosystems, Foster City, CA) as described previously (Aizaki et al., 2004; Murakami et al., 2006). HCV core protein levels in the cells and in the supernatant were quantified using an HCV core enzyme-linked immunosorbent assay (Ortho-Clinical Diagnostics, Tokyo, Japan).

Acknowledgments

We thank Drs. F. V. Chisari (The Scripps Research Institute) and D. Moradpour (Centre Hospitalier Universitaire Vaudois, University of Lausanne) for providing the Huh-7.5.1 cells and anti-NS5B monoclonal antibody, respectively; S. Yoshizaki, M. Kaga, M. Sasaki, and T. Date for their technical assistance, and T. Mizoguchi for secretarial work. This work was supported by a grant-in-aid for Scientific Research from the Japan Society for the Promotion of Science, from the Ministry of Health, Labour and Welfare of Japan, and from the Ministry of Education, Culture, Sports, Science and Technology, and by Research on Health Sciences focusing on Drug Innovation from the Japan Health Sciences Foundation, and by the Program for Promotion of Fundamental Studies in Health Sciences of the National Institute of Biomedical Innovation of Japan.

References

Aizaki, H., Aoki, Y., Harada, T., Ishii, K., Suzuki, T., Nagamori, S., Toda, G., Matsuura, Y., Miyamura, T., 1998. Full-length complementary DNA of hepatitis C virus genome from an infectious blood sample. Hepatology 27 (2), 621–627.

Aizaki, H., Lee, K.J., Sung, V.M., Ishiko, H., Lai, M.M., 2004. Characterization of the hepatitis C virus RNA replication complex associated with lipid rafts. Virology 324 (2), 450–461.

Aizaki, H., Morikawa, K., Fukasawa, M., Hara, H., Inoue, Y., Tani, H., Saito, K., Nishijima, M., Hanada, K., Matsuura, Y., Lai, M.M., Miyamura, T., Wakita, T., Suzuki, T., 2008. Critical role of virion-associated cholesterol and sphingolipid in hepatitis C virus infection. J. Virol. 82 (12), 5715–5724.

Ali, N., Tardif, K.D., Siddiqui, A., 2002. Cell-free replication of the hepatitis C virus subgenomic replicon. J. Virol. 76 (23), 12001–12007.

Burch, A.D., Weller, S.K., 2005. Herpes simplex virus type 1 DNA polymerase requires the mammalian chaperone hsp90 for proper localization to the nucleus. J. Virol. 79 (16), 10740–10749.

Cuéllar, J., Martín-Benito, J., Scheres, S.H., Sousa, R., Moro, F., López-Viñas, E., Gómez-Puertas, P., Muga, A., Carrascosa, J.L., Valpuesta, J.M., 2008. The structure of CCT-Hsc70 NBD suggests a mechanism for Hsp70 delivery of substrates to the chaperonin. Nat. Struct. Mol. Biol. 15 (8), 858–864.

Daikoku, T., Kudoh, A., Sugaya, Y., Iwahori, S., Shirata, N., Isomura, H., Tsurumi, T., 2006. Postreplicative mismatch repair factors are recruited to Epstein–Barr virus replication compartments. J. Biol. Chem. 281 (16), 11422–11430.

De Francesco, R., Migliaccio, G., 2005. Challenges and successes in developing new therapies for hepatitis C. Nature 436 (7053), 953–960.

Dworniczak, B., Mirault, M.E., 1987. Structure and expression of a human gene coding for a 71 kd heat shock 'cognate' protein. Nucleic Acids Res. 15 (13), 5181–5197.

Farr, G.W., Scharl, E.C., Schumacher, R.J., Sondek, S., Horwich, A.L., 1997. Chaperonin-mediated folding in the eukaryotic cytosol proceeds through rounds of release of native and nonnative forms. Cell 89 (6), 927–937.

Feldman, D.E., Spiess, C., Howard, D.E., Frydman, J., 2003. Tumorigenic mutations in VHL disrupt folding in vivo by interfering with chaperonin binding. Mol. Cell 12 (5), 1213–1224.

Fislová, T., Thomas, B., Graef, K.M., Fodor, E., 2010. Association of the influenza virus RNA polymerase subunit PB2 with the host chaperonin CCT. J. Virol. 84 (17), 8691–8699.

Frydman, J., Hartl, F.U., 1996. Principles of chaperone-assisted protein folding: differences between in vitro and in vivo mechanisms. Science 272 (5267), 1497–1502.

Garcin, D., Rochat, S., Kolakofsky, D., 1993. The Tacaribe arenavirus small zinc finger protein is required for both mRNA synthesis and genome replication. J. Virol. 67 (2), 807–812.

Goh, P.Y., Tan, Y.J., Lim, S.P., Tan, Y.H., Lim, S.G., Fuller-Pace, F., Hong, W., 2004. Cellular RNA helicase p68 relocalization and interaction with the hepatitis C virus (HCV) NS5B protein and the potential role of p68 in HCV RNA replication. J. Virol. 78 (10), 5288–5298.

Guo, J.T., Bichko, V.V., Seeger, C., 2001. Effect of alpha interferon on the hepatitis C virus replicon. J. Virol. 75 (18), 8516–8523.

Hamamoto, I., Nishimura, Y., Okamoto, T., Aizaki, H., Liu, M., Mori, Y., Abe, T., Suzuki, T., Lai, M.M., Miyamura, T., Moriishi, K., Matsuura, Y., 2005. Human VAP-B is involved in hepatitis C virus replication through interaction with NS5A and NS5B. J. Virol. 79 (21), 13473–13482.

Hansen, J.L., Long, A.M., Schultz, S.C., 1997. Structure of the RNA-dependent RNA polymerase of poliovirus. Structure 5 (8), 1109–1122.

Hara, H., Aizaki, H., Matsuda, M., Shinkai-Ouchi, F., Inoue, Y., Murakami, K., Shoji, I., Kawakami, H., Matsuura, Y., Lai, M.M., Miyamura, T., Wakita, T., Suzuki, T., 2009. Involvement of creatine kinase B in hepatitis C virus genome replication through interaction with the viral NS4A protein. J. Virol. 83 (10), 5137–5147.

Hardy, R.W., Marcotrigiano, J., Blight, K.J., Majors, J.E., Rice, C.M., 2003. Hepatitis C virus RNA synthesis in a cell-free system isolated from replicon-containing hepatoma cells. J. Virol. 77 (3), 2029–2037.

Hirano, M., Kaneko, S., Yamashita, T., Luo, H., Qin, W., Shirota, Y., Nomura, T., Kobayashi, K., Murakami, S., 2003. Direct interaction between nucleolin and hepatitis C virus NS5B. J. Biol. Chem. 278 (7), 5109–5115.

Hoofnagle, J.H., 2002. Course and outcome of hepatitis C. Hepatology 36 (5 Suppl 1), S21–S29.

Hu, J., Flores, D., Toft, D., Wang, X., Nguyen, D., 2004. Requirement of heat shock protein 90 for human hepatitis B virus reverse transcriptase function. J. Virol. 78 (23), 13122–13131.

Huang, H., Chopra, R., Verdine, G.L., Harrison, S.C., 1998. Structure of a covalently trapped catalytic complex of HIV-1 reverse transcriptase: implications for drug resistance. Science 282 (5394), 1669–1675.

Ichimura, T., Yamamura, H., Sasamoto, K., Tominaga, Y., Taoka, M., Kakiuchi, K., Shinkawa, T., Takahashi, N., Shimada, S., Isobe, T., 2005. 14-3-3 proteins modulate the expression of epithelial Na+ channels by phosphorylation-dependent interaction with Nedd4-2 ubiquitin ligase. J. Biol. Chem. 280 (13), 13187–13194.

Ikeda, M., Yi, M., Li, K., Lemon, S.M., 2002. Selectable subgenomic and genome-length dicistronic RNAs derived from an infectious molecular clone of the HCV-N strain of hepatitis C virus replicate efficiently in cultured Huh7 cells. J. Virol. 76 (6), 2997–3006.

Kampmueller, K.M., Miller, D.J., 2005. The cellular chaperone heat shock protein 90 facilitates Flock House virus RNA replication in *Drosophila* cells. J. Virol. 79 (11), 6827–6837.

Kim, S.J., Kim, J.H., Kim, Y.G., Lim, H.S., Oh, J.W., 2004. Protein kinase C-related kinase 2 regulates hepatitis C virus RNA polymerase function by phosphorylation. J. Biol. Chem. 279 (48), 50031–50041.

Kukihara, H., Moriishi, K., Taguwa, S., Tani, H., Abe, T., Mori, Y., Suzuki, T., Fukuhara, T., Taketomi, A., Maehara, Y., Matsuura, Y., 2009. Human VAP-C negatively regulates hepatitis C virus propagation. J. Virol. 83 (16), 7959–7969.

Kyono, K., Miyashiro, M., Taguchi, I., 2002. Human eukaryotic initiation factor 4AII associates with hepatitis C virus NS5B protein in vitro. Biochem. Biophys. Res. Commun. 292 (3), 659–666.

Laporte, M.G., Jackson, R.W., Draper, T.L., Gaboury, J.A., Galie, K., Herbertz, T., Hussey, A.R., Rippin, S.R., Benetatos, C.A., Chunduru, S.K., Christensen, J.S., Coburn, G.A., Rizzo, C.J., Rhodes, G., O'Connell, J., Howe, A.Y., Mansour, T.S., Collett, M.S., Pevear, D.C., Young, D.C., Gao, T., Tyrrell, D.L., Kneteman, N.M., Burns, C.J., Condon, S.M., 2008. The discovery of pyrano [3, 4-b] indole-based allosteric inhibitors of HCV NS5B polymerase with in vivo activity. ChemMedChem 3 (10), 1508–1515.

Liu, H.M., Aizaki, H., Choi, K.S., Machida, K., Ou, J.J., Lai, M.M., 2009. SYNCRIP (synaptotagmin-binding, cytoplasmic RNA-interacting protein) is a host factor involved in hepatitis C virus RNA replication. Virology 386 (2), 249–256.

Lohmann, V., Körner, F., Herian, U., Bartenschlager, R., 1997. Biochemical properties of hepatitis C virus NS5B RNA-dependent RNA polymerase and identification of amino acid sequence motifs essential for enzymatic activity. J. Virol. 71 (11), 8416–8428.

Lohmann, V., Roos, A., Körner, F., Koch, J.O., Bartenschlager, R., 2000. Biochemical and structural analysis of the NS5B RNA-dependent RNA polymerase of the hepatitis C virus. J. Viral Hepat. 7 (3), 167–174.

Manns, M.P., Wedemeyer, H., Cornberg, M., 2006. Treating viral hepatitis C: efficacy, side effects, and complications. Gut 55 (9), 1350–1359.

Meyer, A.S., Gillespie, J.R., Walther, D., Millet, I.S., Doniach, S., Frydman, J., 2003. Closing the folding chamber of the eukaryotic chaperonin requires the transition state of ATP hydrolysis. Cell 113 (3), 369–381.

Momose, F., Naito, T., Yano, K., Sugimoto, S., Morikawa, Y., Nagata, K., 2002. Identification of Hsp90 as a stimulatory host factor involved in influenza virus RNA synthesis. J. Biol. Chem. 277 (47), 45306–45314.

Moradpour, D., Bieck, E., Hügle, T., Wels, W., Wu, J.Z., Hong, Z., Blum, H.E., Bartenschlager, R., 2002. Functional properties of a monoclonal antibody inhibiting the hepatitis C virus RNA-dependent RNA polymerase. J. Biol. Chem. 277 (1), 593–601.

Moriishi, K., Matsuura, Y., 2007. Host factors involved in the replication of hepatitis C virus. Rev. Med. Virol. 17 (5), 343–354.

Murakami, K., Ishii, K., Ishihara, Y., Yoshizaki, S., Tanaka, K., Gotoh, Y., Aizaki, H., Kohara, M., Yoshioka, H., Mori, Y., Manabe, N., Shoji, I., Sata, T., Bartenschlager, R., Matsuura, Y., Miyamura, T., Suzuki, T., 2006. Production of infectious hepatitis C virus particles in three-dimensional cultures of the cell line carrying the genome-length dicistronic viral RNA of genotype 1b. Virology 351 (2), 381–392.

Naito, T., Momose, F., Kawaguchi, A., Nagata, K., 2007. Involvement of Hsp90 in assembly and nuclear import of influenza virus RNA polymerase subunits. J. Virol. 81 (3), 1339–1349.

Nakagawa, S., Umehara, T., Matsuda, C., Kuge, S., Sudoh, M., Kohara, M., 2007. Hsp90 inhibitors suppress HCV replication in replicon cells and humanized liver mice. Biochem. Biophys. Res. Commun. 353 (4), 882–888.
Nelson, H.B., Tang, H., 2006. Effect of cell growth on hepatitis C virus (HCV) replication and a mechanism of cell confluence-based inhibition of HCV RNA and protein expression. J. Virol. 80 (3), 1181–1190.
Niwa, H., Yamamura, K., Miyazaki, J., 1991. Efficient selection for high-expression transfectants with a novel eukaryotic vector. Gene 108 (2), 193–199.
Okamoto, T., Nishimura, Y., Ichimura, T., Suzuki, K., Miyamura, T., Suzuki, T., Moriishi, K., Matsuura, Y., 2006. Hepatitis C virus RNA replication is regulated by FKBP8 and Hsp90. EMBO J. 25 (20), 5015–5025.
Okamoto, T., Omori, H., Kaname, Y., Abe, T., Nishimura, Y., Suzuki, T., Miyamura, T., Yoshimori, T., Moriishi, K., Matsuura, Y., 2008. A single-amino-acid mutation in hepatitis C virus NS5A disrupting FKBP8 interaction impairs viral replication. J. Virol. 82 (7), 3480–3489.
Parent, R., Qu, X., Petit, M.A., Beretta, L., 2009. The heat shock cognate protein 70 is associated with hepatitis C virus particles and modulates virus infectivity. Hepatology 49 (6), 1798–1809.
Pietschmann, T., Lohmann, V., Rutter, G., Kurpanek, K., Bartenschlager, R., 2001. Characterization of cell lines carrying self-replicating hepatitis C virus RNAs. J. Virol. 75 (3), 1252–1264.
Pietschmann, T., Lohmann, V., Kaul, A., Krieger, N., Rinck, G., Rutter, G., Strand, D., Bartenschlager, R., 2002. Persistent and transient replication of full-length hepatitis C virus genomes in cell culture. J. Virol. 76 (8), 4008–4021.
Saito, I., Miyamura, T., Ohbayashi, A., Harada, H., Katayama, T., Kikuchi, S., Watanabe, Y., Koi, S., Onji, M., Ohta, Y., Choo, Q.L., Houghton, M., Kuo, G., 1990. Hepatitis C virus infection is associated with the development of hepatocellular carcinoma. Proc. Natl Acad. Sci. USA 87 (17), 6547–6549.
Seeff, L.B., Hoofnagle, J.H., 2003. Appendix: the National Institutes of Health Consensus Development Conference: management of hepatitis C 2002. Clin. Liver Dis. 7 (1), 261–287.
Shi, S.T., Lee, K.J., Aizaki, H., Hwang, S.B., Lai, M.M., 2003. Hepatitis C virus RNA replication occurs on a detergent-resistant membrane that cofractionates with caveolin-2. J. Virol. 77 (7), 4160–4168.
Shimakami, T., Honda, M., Kusakawa, T., Murata, T., Shimotohno, K., Kaneko, S., Murakami, S., 2006. Effect of hepatitis C virus (HCV) NS5B-nucleolin interaction on HCV replication with HCV subgenomic replicon. J. Virol. 80 (7), 3332–3340.
Shirakura, M., Murakami, K., Ichimura, T., Suzuki, R., Shimoji, T., Fukuda, K., Abe, K., Sato, S., Fukasawa, M., Yamakawa, Y., Nishijima, M., Moriishi, K., Matsuura, Y., Wakita, T., Suzuki, T., Howley, P.M., Miyamura, T., Shoji, I., 2007. E6AP ubiquitin ligase mediates ubiquitylation and degradation of hepatitis C virus core protein. J. Virol. 81 (3), 1174–1185.
Suzuki, T., Ishii, K., Aizaki, H., Wakita, T., 2007. Hepatitis C viral life cycle. Adv. Drug Deliv. Rev. 59 (12), 1200–1212.
Taguwa, S., Okamoto, T., Abe, T., Mori, Y., Suzuki, T., Moriishi, K., Matsuura, Y., 2008. Human butyrate-induced transcript 1 interacts with hepatitis C virus NS5A and regulates viral replication. J. Virol. 82 (6), 2631–2641.
Taguwa, S., Kambara, H., Omori, H., Tani, H., Abe, T., Mori, Y., Suzuki, T., Yoshimori, T., Moriishi, K., Matsuura, Y., 2009. Cochaperone activity of human butyrate-induced transcript 1 facilitates hepatitis C virus replication through an Hsp90-dependent pathway. J. Virol. 83 (20), 10427–10436.
Tian, G., Vainberg, I.E., Tap, W.D., Lewis, S.A., Cowan, N.J., 1995. Specificity in chaperonin-mediated protein folding. Nature 375 (6528), 250–253.
Tu, H., Gao, L., Shi, S.T., Taylor, D.R., Yang, T., Mircheff, A.K., Wen, Y., Gorbalenya, A.E., Hwang, S.B., Lai, M.M., 1999. Hepatitis C virus RNA polymerase and NS5A complex with a SNARE-like protein. Virology 263 (1), 30–41.
Ujino, S., Yamaguchi, S., Shimotohno, K., Takaku, H., 2009. Heatshock protein 90 is essential for stabilization of the hepatitis C virus nonstructural protein NS3. J. Biol. Chem. 284 (11), 6841–6846.
Valpuesta, J.M., Martín-Benitoa, J., Gómez-Puertasa, P., Carrascosaa, J.L., Willison, K.R., 2002. Structure and function of a protein folding machine: the eukaryotic cytosolic chaperonin CCT. FEBS Lett. 529 (1), 11–16.
Wakita, T., Pietschmann, T., Kato, T., Date, T., Miyamoto, M., Zhao, Z., Murthy, K., Habermann, A., Krausslich, H.G., Mizokami, M., Bartenschlager, R., Liang, T.J., 2005. Production of infectious hepatitis C virus in tissue culture from a cloned viral genome. Nat. Med. 11 (7), 791–796.
Watashi, K., Ishii, N., Hijikata, M., Inoue, D., Murata, T., Miyanari, Y., Shimotohno, K., 2005. Cyclophilin B is a functional regulator of hepatitis C virus RNA polymerase. Mol. Cell 19 (1), 111–122.
Weng, L., Du, J., Zhou, J., Ding, J., Wakita, T., Kohara, M., Toyoda, T., 2009. Modification of hepatitis C virus 1b RNA polymerase to make a highly active JFH1-type polymerase by mutation of the thumb domain. Arch. Virol. 154 (5), 765–773.
Yaffe, M.B., Farr, G.W., Miklos, D., Horwich, A.L., Sternlicht, M.L., Sternlicht, H., 1992. TCP1 complex is a molecular chaperone in tubulin biogenesis. Nature 358 (6383), 245–248.
Yam, A.Y., Xia, Y., Lin, H.T., Burlingame, A., Gerstein, M., Frydman, J., 2008. Defining the TRiC/CCT interactome links chaperonin function to stabilization of newly made proteins with complex topologies. Nat. Struct. Mol. Biol. 15 (12), 1255–1262.
Yanagida, M., Miura, Y., Yagasaki, K., Taoka, M., Isobe, T., Takahashi, N., 2000. Matrix assisted laser desorption/ionization-time of flight-mass spectrometry analysis of proteins detected by anti-phosphotyrosine antibody on two-dimensional-gels of fibroblast cell lysates after tumor necrosis factor-alpha stimulation. Electorophoresis 21 (9), 1890–1898.
Yang, G., Pevear, D.C., Collett, M.S., Chunduru, S., Young, D.C., Benetatos, C., Jordan, R., 2004. Newly synthesized hepatitis C virus replicon RNA is protected from nuclease activity by a protease-sensitive factor(s). J. Virol. 78 (18), 10202–10205.

ARTICLE
Journal of Cellular Biochemistry 111:676–685 (2010)
Journal of Cellular Biochemistry

E6AP Ubiquitin Ligase Mediates Ubiquitin-Dependent Degradation of Peroxiredoxin 1

Junichi Nasu,[1,2] Kyoko Murakami,[1] Shoji Miyagawa,[3] Ryosuke Yamashita,[3] Tohru Ichimura,[4] Takaji Wakita,[1] Hak Hotta,[3] Tatsuo Miyamura,[1] Tetsuro Suzuki,[1] Tazuko Satoh,[2] and Ikuo Shoji[1,3*]

[1]*Department of Virology II, National Institute of Infectious Diseases, Shinjuku-ku, Tokyo, Japan*

[2]*Department of Oral and Maxillofacial Surgery, School of Life Dentistry at Tokyo, the Nippon Dental University, Chiyoda-ku, Tokyo, Japan*

[3]*Division of Microbiology, Center for Infectious Diseases, Kobe University Graduate School of Medicine, Kobe, Hyogo, Japan*

[4]*Department of Applied Chemistry, National Defense Academy, Yokosuka, Kanagawa, Japan*

ABSTRACT

E6-associated protein (E6AP) is a cellular ubiquitin protein ligase that mediates ubiquitylation and degradation of tumor suppressor p53 in conjunction with the high-risk human papillomavirus E6 protein. We previously reported that E6AP targets annexin A1 protein for ubiquitin-dependent proteasomal degradation. To gain a better understanding of the physiological function of E6AP, we have been seeking to identify novel substrates of E6AP. Here, we identified peroxiredoxin 1 (Prx1) as a novel E6AP-binding protein using a tandem affinity purification procedure coupled with mass spectrometry. Prx1 is a 25-kDa member of the Prx family, a ubiquitous family of antioxidant peroxidases that regulate many cellular processes through intracellular oxidative signal transduction pathways. Immunoprecipitation analysis showed that E6AP binds Prx1 in vivo. Pull-down experiments showed that E6AP binds Prx1 in vitro. Ectopic expression of E6AP enhanced the degradation of Prx1 in vivo. In vivo and in vitro ubiquitylation assays revealed that E6AP promoted polyubiquitylation of Prx1. RNAi-mediated downregulation of endogenous E6AP increased the level of endogenous Prx1 protein. Taken together, our data suggest that E6AP mediates the ubiquitin-dependent proteasomal degradation of Prx1. Our findings raise a possibility that E6AP may play a role in regulating Prx1-dependent intracellular oxidative signal transduction pathways. J. Cell. Biochem. 111: 676–685, 2010.

KEY WORDS: E6AP; Prx1; UBIQUITIN; DEGRADATION

E6-associated protein (E6AP) is the prototype of a family of ubiquitin ligases called HECT domain ubiquitin ligases, all of which contain a domain homologous to the E6AP carboxyl terminus [Huibregtse et al., 1995]. E6AP was initially identified as the cellular factor that stimulates ubiquitin-dependent degradation of the tumor suppressor p53 in conjunction with the E6 protein of cervical cancer-associated human papillomavirus (HPV) types 16 and 18 [Huibregtse et al., 1993; Scheffner et al., 1994]. The E6–E6AP complex functions as an E3 ubiquitin ligase in the ubiquitylation of p53 [Scheffner et al., 1993]. Known substrates of the E6–E6AP complex include the tumor suppressor p53 [Scheffner et al., 1993], the PDZ domain-containing protein Scribble [Nakagawa and Huibregtse, 2000], and NFX1-91, a transcriptional repressor of the gene encoding hTERT [Gewin et al., 2004]. The ability of E6 to

Abbreviations: E6AP, E6-associated protein; Prx, peroxiredoxin; HPV, human papillomavirus; MS, mass spectrometry; MAb, monoclonal antibody; PAb, polyclonal antibody; GAPDH, glyceraldehydes-3-phosphate dehydrogenase; CHX, cycloheximide.

Grant sponsor: The Nippon Dental University; Grant sponsor: Japan Health Sciences Foundation; Grant sponsor: Ministry of Health, Labour, and Welfare; Grant sponsor: Ministry of Education, Science and Culture of Japan; Grant sponsor: Program for Promotion of Fundamental Studies in Health Sciences of the National Institute of Biomedical Innovation (NIBIO), Japan.

*Correspondence to: Dr. Ikuo Shoji, MD, PhD, Division of Microbiology, Center for Infectious Diseases, Kobe University Graduate School of Medicine, 7-5-1 Kusunoki-cho, Chuo-ku, Kobe, Hyogo 650-0017, Japan.
E-mail: ishoji@med.kobe-u.ac.jp

Received 7 March 2010; Accepted 15 June 2010 • DOI 10.1002/jcb.22752 • © 2010 Wiley-Liss, Inc.
Published online 29 June 2010 in Wiley Online Library (wileyonlinelibrary.com).

utilize E6AP to target p53 and other cellular proteins for degradation contributes to its oncogenic functions [Matentzoglu and Scheffner, 2008]. Interestingly, E6AP is not involved in the ubiquitylation of p53 in the absence of E6 [Talis et al., 1998].

In an attempt to understand the physiological function of E6AP, several potential E6-independent substrates for E6AP have been identified, such as HHR23A and HHR23B (the human orthologs of *Saccharomyces cerevisae* Rad23) [Kumar et al., 1999], Blk (a member of the Src family kinases) [Oda et al., 1999], Mcm7 (which is involved in DNA replication) [Kuhne and Banks, 1998], trihydrophobin 1 [Yang et al., 2007], and AIB1 (a steroid receptor coactivator) [Mani et al., 2006]. We previously reported that E6AP mediates ubiquitylation and degradation of annexin A1 in a Ca^{2+}-dependent manner [Shimoji et al., 2009].

Some patients with Angelman syndrome, a severe neurological disorder linked to E6AP, have mutations within the catalytic cleft that have been shown to reduce E6AP ubiquitin ligase activity [Kishino et al., 1997; Matsuura et al., 1997; Cooper et al., 2004]. Despite the significant progress in the study of Angelman syndrome-associated E6AP mutations, none of the identified E6AP substrates have been directly linked to the disorder. Much research is still needed to fully understand the functional links between lack of E6AP expression and clinical manifestations of Angelman syndrome [Dan, 2009]. We previously reported that E6AP mediates ubiquitin-dependent proteasomal degradation of hepatitis C virus (HCV) core protein, thereby affecting the production of HCV particles [Shirakura et al., 2007; Suzuki et al., 2009]. It is becoming increasingly clear that E6AP plays important roles in human diseases, such as cervical cancer, Angelman syndrome, and hepatitis C [Scheffner et al., 1993; Kishino et al., 1997; Shirakura et al., 2007].

In this study, we attempted to identify the novel functions of E6AP. We screened for potential binding partners for E6AP. A tandem affinity purification procedure coupled with mass spectrometry analysis identified peroxiredoxin 1 (Prx1) as a novel binding partner for E6AP. We provide evidence suggesting that E6AP mediates the ubiquitin-dependent proteasomal degradation of Prx1.

MATERIALS AND METHODS

CELL CULTURE AND TRANSFECTION

Human embryonic kidney (HEK) 293T cells were cultured in Dulbecco's modified Eagle's medium (DMEM; Sigma–Aldrich, St. Louis, MO) supplemented with 50 IU/ml penicillin, 50 μg/ml streptomycin (Invitrogen, Carlsbad, CA), and 10% (v/v) fetal bovine serum (FBS; JRH Biosciences, Lenexa, KS) at 37°C in a 5% CO_2 incubator. HEK293T cells were transfected with plasmid DNA using TransIT-LT1 (Mirus, Madison, WI).

PLASMIDS AND RECOMBINANT BACULOVIRUSES

To make a fusion protein consisting of hexahistidine (His_6)-tag fused to the N-terminus of Prx1 in *Escherichia coli*, pET17b-Prx1 [Kang et al., 1998] was digested with *Nde*I and *Bam*HI, and a Prx1 fragment was subcloned into the *Nde*I-Bpu1120I site of pET19b, resulting in pET19b-Prx1. The expression plasmid pET19b-Prx2 was constructed similarly. The plasmids, pET17b-Prx1 and pET17b-Prx2, were kind gifts from Dr. S.G. Rhee, Ewha Women's University, Korea.

To express the Prx1 protein as a FLAG-tagged fusion protein in mammalian cells, pCAG-FLAG-Prx1 was constructed as follows. The DNA fragment of Prx1 was amplified from pET17b-PrxI by polymerase chain reaction (PCR) using two oligonucleotides, 5′-GCGGCCGCCCACCATGGACTACAAAGACGATGACGATAAAGG-AGGCGGCGGATCCATGTCTTCAGGAAATGC-3′ and 5′-AGATCTT-CACTTCTGCTTGGAG-3′. To express FLAG-tagged Prx2 protein in mammalian cells, the DNA fragment of Prx2 was amplified from pET17b-Prx2 by PCR using two oligonucleotides, 5′-GCGGCCG-CCCACCATGGACTACAAAGACGATGACGATAAAGGAGGCGGCG-GATCCATGGCCTCCGGTAACGC-3′ and 5′-AGATCTCTAATTGTG-TTTGGAG-3′. The amplified PCR fragments were subcloned into pGEM T-Easy (Promega, Madison, WI) and verified by sequencing. Then the Prx1 and Prx2 gene fragments were digested with *Not*I and *Bgl*II, and ligated into the *Not*I–*Bgl*II site of pCAG-MCS2 [Shirakura et al., 2007]. The MEF-tag cassette (containing Myc-tag, the tobacco etch virus protease cleavage site, and FLAG-tag) was fused to the N-terminus of the cDNA encoding E6AP [Ichimura et al., 2005; Shirakura et al., 2007]. MEF-tagged E6AP and MEF-tagged E6AP C-A were subcloned into pcDNA3, pCAGGS, and pVL1392. pCAG-HA-E6AP, pCAG-HA-E6AP C-A, and pCAG-HA-Nedd4 were described previously [Shirakura et al., 2007; Shimoji et al., 2009]. The ubiquitin expression plasmids, pRK5-HA-Ubiquitin wild type (WT), pRK5-HA-Ubiquitin-K48R, and pRK5-HA-Ubiquitin-K48 [Lim et al., 2005], were provided by Dr. T. Dawson (Johns Hopkins University, MD).

ANTIBODIES

The mouse monoclonal antibodies (MAbs) used in this study were anti-hemagglutinin (HA) MAb (12CA5; Roche, Mannheim, Germany), anti-HA MAb (16B12; Covance, Princeton, NJ), anti-FLAG M2 mouse MAb (Sigma–Aldrich), anti-glyceraldehyde-3-phosphate dehydrogenase (GAPDH) MAb (Chemicon, Temecula, CA), anti-E6AP MAb (E6AP-330; Sigma–Aldrich), and anti-polyhistidine (His-1) MAb (Sigma–Aldrich). The c-Myc tagged protein mild purification kit (MBL) was used for immunoprecipitation. The polyclonal antibodies (PAbs) used in this study were anti-HA rabbit PAb (Y-11; Santa Cruz Biotechnology, Santa Cruz, CA), anti-FLAG rabbit PAb (F7425; Sigma–Aldrich), anti-Prx1 rabbit PAb (ab16805-100) (Abcam, Cambridge, Oxford), and anti-GST goat PAb (Amersham, Buckinghamshire, UK).

EXPRESSION AND PURIFICATION OF RECOMBINANT PROTEINS

E. coli BL21 (DE3) cells were transformed with plasmids expressing His_6-tagged protein and grown at 37°C. Expression of the fusion protein was induced by 1 mM isopropyl-β-D-thiogalactopyranoside (IPTG) at 25°C for 4 h. Bacteria were harvested, suspended in lysis buffer [50 mM Na_2HPO_4, 300 mM NaCl, 5 mM Imidazole, 0.1% Triton X-100, protease inhibitor cocktail (Complete EDTA-free; Roche)], and sonicated on ice. His_6-tagged proteins were purified on Ni-NTA beads (Qiagen, Hilden, Germany) according to the manufacturer's protocols. The MEF-E6AP and MEF-E6AP C-A were purified on anti-FLAG M2 agarose beads (Sigma–Aldrich) as described previously [Shirakura et al., 2007].

PURIFICATION OF E6AP-BINDING PROTEINS BY MEF PURIFICATION PROCEDURE

HEK293T cells were transfected with the plasmid expressing MEF-E6AP C-A by the calcium phosphate precipitation method, and the E6AP-binding proteins were recovered following the procedure described previously [Ichimura et al., 2005]. The inactive form of E6AP was expressed to inhibit ubiquitin-dependent degradation of potential substrates. Bound proteins were separated by 7.5% sodium dodecyl sulfate-polyacrylamide gel electrophoresis (SDS–PAGE) and visualized by silver staining. The stained bands were excised and digested in the gel with lysylendoprotease-C (Lys-C), and the resulting peptide mixtures were analyzed using a direct nanoflow liquid chromatography-tandem mass spectrometry (MS/MS) system, equipped with an electrospray interface reversed-phase column, a nanoflow gradient device, a high-resolution Q-time of flight hybrid mass spectrometer (Q-TOF2; Micromass, Manchester, UK), and an automated data analysis system [Natsume et al., 2002; Shirakura et al., 2007]. All the MS/MS spectra were searched against the nonredundant protein sequence database maintained at the National Center for Biotechnology Information using the Mascot program (Matrix Science, London, UK) to identify proteins. The MS/MS signal assignments were also confirmed manually.

Ni-NTA PULL-DOWN ASSAY

For Ni-NTA pull-down assays, purified MEF-E6AP was incubated with His_6-Prx proteins immobilized on Ni-NTA agarose beads (Qiagen) in 1 ml of the binding buffer [50 mM Tris–HCl (pH 7.5), 10% glycerol, 1% Triton X-100, 150 mM NaCl, 5 μM $ZnCl_2$, 1 mM Na_3VO_4, 10 mM EGTA, protease inhibitor cocktail (Complete EDTA-free)] at 4°C for 30 min. The beads were washed four times with wash buffer [50 mM Na_2HPO_4, 300 mM NaCl, 50 mM Imidazole, 0.1% Triton X-100, protease inhibitor cocktail (Complete EDTA-free)], and the pull-down complexes were separated by SDS–PAGE on 12.5% polyacrylamide gels and analyzed by immunoblotting with anti-FLAG MAb and anti-polyhistidine (His-1) MAb.

IMMUNOFLUORESCENCE MICROSCOPY

Cells were transfected with pCAG-HA-E6AP C-A and pCAG-FLAG-Prx1 using TransIT-LT1 according to the manufacturer's instructions. Transfected cells grown on collagen-coated coverslips were washed with PBS, fixed with 4% paraformaldehyde for 30 min at 4°C, and permeabilized with PBS containing 2% FCS and 0.3% Triton X-100. Cells were incubated with anti-HA mouse MAb and anti-FLAG rabbit PAb as primary antibodies, washed, and incubated with Alexa Fluor 488 goat anti-mouse IgG (Molecular Probes, Eugene, OR) and Alexa Fluor 555 goat anti-rabbit IgG (Molecular Probes) as secondary antibodies. Then, the cells were washed with PBS, mounted on glass slides, and examined with a BZ-8000 microscope (Keyence).

siRNA TRANSFECTION

HEK293T cells (3×10^5 cells in a six-well plate) were transfected with 40 pmol of either E6AP-specific small interfering RNA (siRNA; Sigma–Aldrich), or scramble negative-control siRNA duplexes (Sigma–Aldrich) using HiPerFect transfection reagent (Qiagen) following the manufacturer's instructions. The E6AP-siRNA target sequences were as follows:

siE6AP-1 (sense), 5′-GGGUCUACACCAGAUUGCUTT-3′; scramble negative control (siCont-1, sense), 5′-UUGCGGGUCUAAUCACCGATT-3′ [Shirakura et al., 2007].

IN VIVO UBIQUITYLATION ASSAY

In vivo ubiquitylation assays were performed essentially as described previously [Shirakura et al., 2007]. Where indicated, cells were treated with 25 μM MG132 (Calbiochem, La Jolla, CA) or with dimethylsulfoxide (DMSO; control) for 30 min prior to collection. FLAG-Prx1 was immunoprecipitated with anti-FLAG MAb. Immunoprecipitates were analyzed by immunoblotting, using either anti-HA PAb or anti-FLAG MAb to detect ubiquitylated Prx1.

IN VITRO UBIQUITYLATION ASSAY

In vitro ubiquitylation assays were performed essentially as described previously [Shirakura et al., 2007]. For in vitro ubiquitylation of Prx1, purified His_6–Prx1 was used as a substrate. Assays were done in 40-μl volumes containing 20 mM Tris–HCl, pH 7.6, 50 mM NaCl, 5 mM $MgCl_2$, 5 mM ATP, 8 μg of bovine ubiquitin (Sigma–Aldrich), 0.1 mM DTT, 200 ng of mouse E1, 200 ng of E2 (UbcH7), and 0.5 μg of MEF-E6AP. The reaction mixtures were incubated at 37°C for 120 min followed by immunoprecipitation with anti-Prx1 PAb. The samples were analyzed by immunoblotting with anti-Ub MAb.

RESULTS

IDENTIFICATION OF Prx1 AS A BINDING PARTNER FOR E6AP

To identify novel substrates for E6AP, we screened for E6AP-binding proteins using a tandem affinity purification procedure with a tandem tag (known as MEF-tag) [Ichimura et al., 2005; Shirakura et al., 2007]. Seven proteins were reproducibly detected from lysed cells transfected with MEF-E6AP C-A (Fig. 1A, lane 2), but none were recovered from lysed control cells transfected with empty vector alone (Fig. 1A, lane 1). To identify the proteins, silver-stained bands were excised from the gel, digested with Lys-C, and analyzed using a direct nanoflow liquid chromatography-MS/MS system. One of these bands, migrating at 25 kDa (Fig. 1A, lane 2, No. 7), was identified as Prx1 based on two independent MS spectra (Fig. 1B,C). To confirm the proteomic identification of Prx1, HEK293T cells were transfected with MEF-E6AP C-A plasmid or empty plasmid. The cells were lysed and immunoprecipitated with anti-Myc MAb or control IgG. Endogenous Prx1 was co-immunoprecipitated with anti-Myc MAb, suggesting that E6AP binds endogenous Prx1 (Fig. 1D, lane 4).

IN VIVO INTERACTION BETWEEN Prx1 AND E6AP

To determine whether E6AP specifically interacts with Prx1, HA-E6AP plasmid was introduced into HEK293T cells together with either FLAG-Prx1 plasmid or FLAG-Prx2 plasmid. Prx1 and Prx2 share 77.4% sequence identity at the protein level. Cells were lysed and immunoprecipitated with anti-HA MAb, anti-FLAG MAb, or

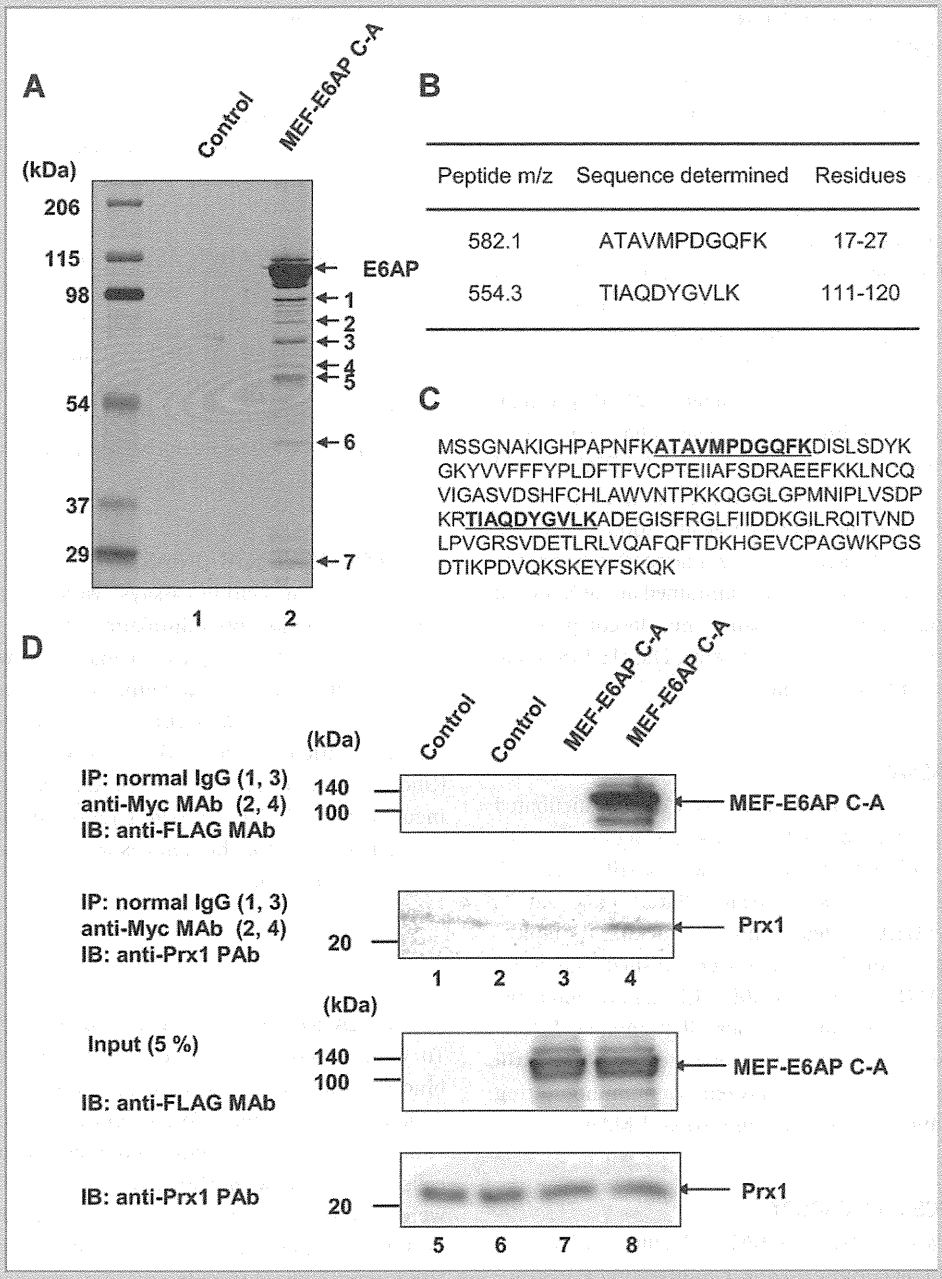

Fig. 1. Identification of Prx1 as a binding partner for E6AP. A: Prx1 interacts with E6AP in vivo. HEK293T cells were transfected with pcDNA3-MEF-E6AP C-A or empty plasmid, incubated for 48 h, and then harvested. The expressed MEF-E6AP C-A and binding proteins were recovered using the MEF purification procedure. Proteins bound to the MEF-E6AP C-A immobilized on anti-FLAG beads were dissociated with FLAG peptides, resolved by 7.5% SDS-PAGE, and visualized by silver staining. Control experiments were performed using HEK293T cells transfected with vector alone. Bound proteins were detected by SDS-PAGE and silver staining. Molecular weight markers are indicated as well as the position of p25 (No. 7), which likely corresponds to Prx1. B: Peptide masses were identified by tandem mass spectrometry. The protein was Prx1 (GenBank accession No. BC021683). C: Corresponding amino acids of Prx1 (peptides in bold print). D: HEK293T cells were co-transfected with MEF-E6AP C-A plasmid. Control experiments were performed using HEK293T cells transfected with vector alone. Cell lysates were immunoprecipitated with anti-Myc MAb or normal mouse IgG (lanes 1–4), eluted with c-Myc tag peptide. Eluates were analyzed by immunoblotting with anti-FLAG MAb or anti-Prx1 PAb. The input samples were separated by SDS-PAGE and analyzed by immunoblotting with anti-FLAG MAb or anti-Prx1 PAb (lanes 5–8). The positions of Prx1 and MEF-E6AP C-A are indicated by arrows. IB, immunoblot; IP, immunoprecipitation.

normal IgG (Fig. 2A, lanes 1–6). FLAG-Prx1 but not FLAG-Prx2 was co-immunoprecipitated with anti-HA MAb (Fig. 2A, lower panel, lanes 1 and 2). Conversely, HA-E6AP was co-immunoprecipitated with FLAG-Prx1 but not FLAG-Prx2 using anti-FLAG MAb (Fig. 2A, upper panel, lanes 3 and 4). These results suggest that E6AP specifically interacts with Prx1.

To determine whether Prx1 and E6AP co-localize in the cells, immunofluorescence microscopy analysis was performed in HEK293T cells. There was no staining without primary antibodies (data not shown). The immunofluorescence study showed that E6AP and Prx1 mainly localize in the cytoplasm and that E6AP and Prx1 co-localize in the cytoplasm (Fig. 2B, Merge).

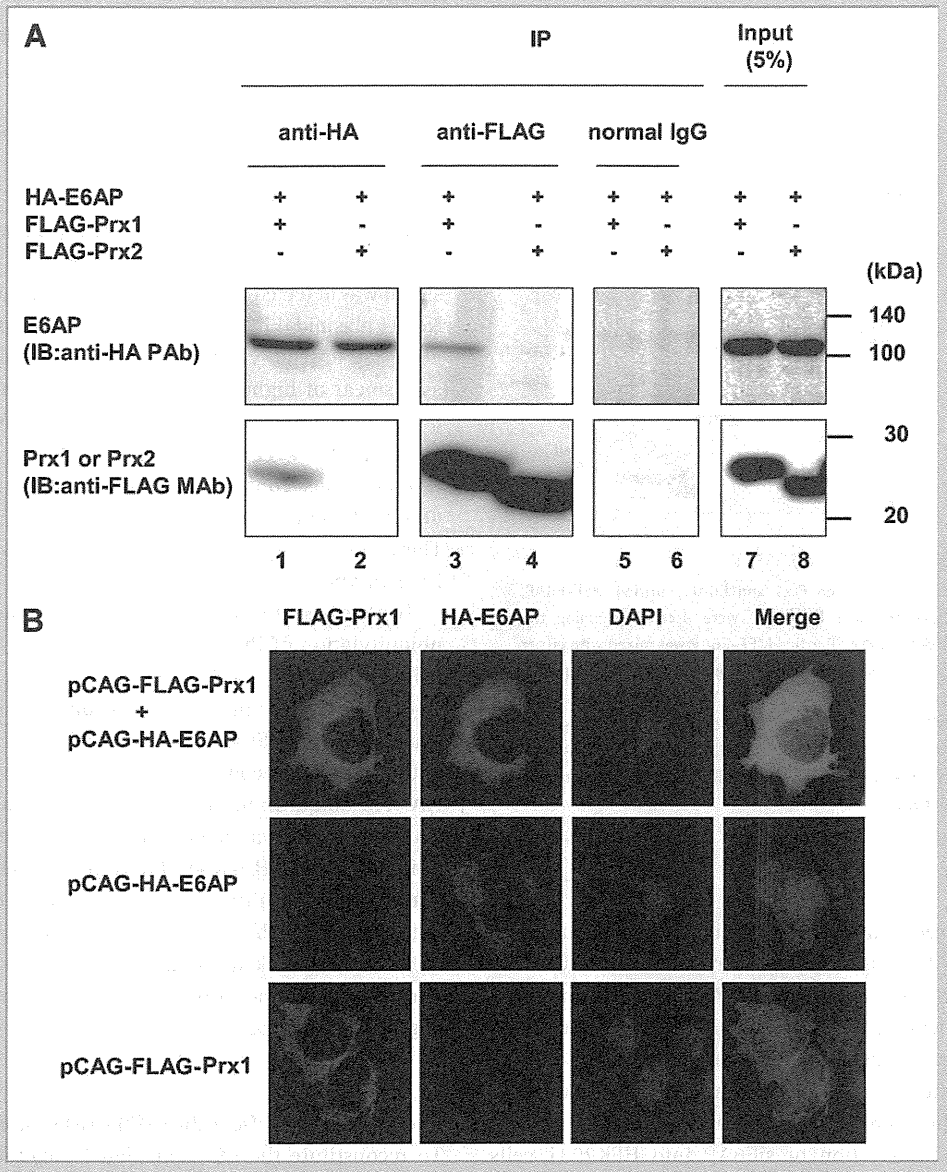

Fig. 2. In vivo interaction between Prx1 and E6AP. A: HEK293T cells were co-transfected with pCAG-HA-E6AP together with either pCAG-FLAG-Prx1 or pCAG-FLAG-Prx2. Cell lysates were immunoprecipitated with anti-HA mouse MAb, anti-FLAG mouse MAb, or normal mouse IgG and analyzed by immunoblotting with anti-HA PAb or anti-FLAG MAb. B: HEK293T cells were transfected with either HA-E6AP plasmid or FLAG-Prx1 plasmid, grown on coverslips, fixed, and processed for double-label immunofluorescence for HA-E6AP or FLAG-Prx1. All the samples were examined with a BZ-8000 microscope (Keyence).

IN VITRO INTERACTION BETWEEN Prx1 AND E6AP

To determine whether E6AP interacts with Prx1 in vitro, purified recombinant MEF-E6AP, MEF-annexin A1 expressed in insect cells using a baculovirus system and purified recombinant His_6-Prx1 and His_6-Prx2 expressed in *E. coli* were used. The His_6-tagged Prx proteins were mixed with either MEF-E6AP or MEF-annexin A1, incubated, pulled down with Ni-NTA agarose, and analyzed by immunoblotting with anti-FLAG MAb (Fig. 3, upper panel) or anti-polyhistidine MAb (Fig. 3, middle panel). MEF-annexin A1 served as a negative control to confirm that MEF-tag does not bind Prx1. MEF-E6AP was pulled down with Prx1, but not with Prx2 (Fig. 3, lanes 1 and 3), whereas annexin A1 was not pulled down with either Prx1 or Prx2 (Fig. 3, lanes 2 and 4). These results suggest that E6AP directly and specifically binds Prx1 in vitro.

E6AP DECREASES STEADY-STATE LEVELS OF Prx1 IN HEK293T CELLS

One of the characteristic features of HECT domain ubiquitin ligases is their direct association with their substrates. Thus, we hypothesized that E6AP would function as an E3 ubiquitin ligase for Prx1. We assessed the effects of E6AP on the steady-state levels of Prx1 in HEK293T cells. FLAG-Prx1 together with HA-tagged E6AP, catalytically inactive E6AP, E6AP C-A, or Nedd4 (another HECT domain ubiquitin ligase) was introduced into HEK293T cells, and the levels of Prx1 were examined by immunoblotting. The steady-state

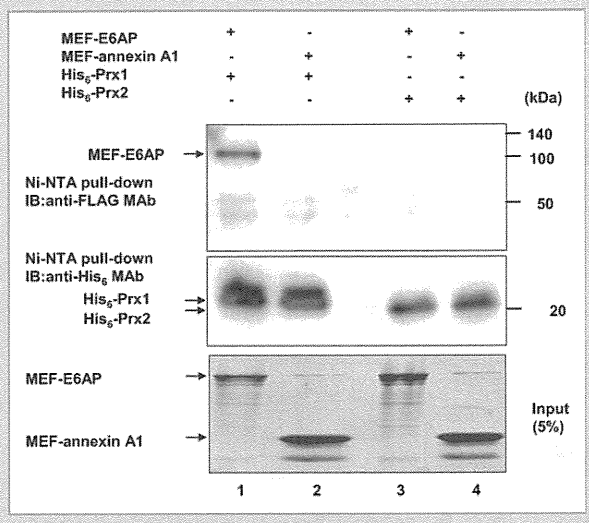

Fig. 3. In vitro interaction between Prx1 and E6AP. Purified MEF-E6AP, MEF-Annexin A1, His_6-Prx1, and His_6-Prx2 were used to examine the interaction between E6AP and Prxs. Purified MEF-E6AP was mixed with either His_6-Prx1 or His_6-Prx2, incubated, and pulled down with Ni-NTA agarose. MEF-Annexin A1 served as a negative control. The bound proteins were separated by SDS-PAGE and analyzed by immunoblotting with anti-FLAG MAb (upper panel) or anti-His_6 MAb (middle panel). The input MEF-E6AP and MEF-annexin A1 were separated by SDS-PAGE and stained with Coomassie brilliant blue (lower panel).

levels of Prx1 decreased with an increase in the amount of E6AP plasmid (Fig. 4A lanes 1–3, Fig. 4B). However, neither E6AP C-A nor Nedd4 decreased the steady-state levels of Prx1 (Fig. 4A lanes 4–6 and 7–9, Fig. 4B), indicating that E6AP specifically decreases Prx1.

To determine if endogenous E6AP is critical for the degradation of endogenous Prx1 in the cells, the expression of E6AP was knocked down by siRNA and the expression of Prx1 and E6AP was analyzed by immunoblotting. Transfection of siE6AP into HEK293T cells resulted in a decrease in E6AP levels by 97% (Fig. 4C, upper panel, lane 2). Knock-down of endogenous E6AP resulted in accumulation of endogenous Prx1 (Fig. 4C, lane 2, middle panel), suggesting that endogenous E6AP plays a role in the proteolysis of endogenous Prx1.

To further investigate if the E6AP-induced reduction of Prx1 is dependent on the proteasome, we examined the effects of the proteasome inhibitor clasto-lactacystin and the lysosomal enzyme inhibitors, E-64d and Pepstatin A, on the level of Prx1. Clasto-lactacystin was used to examine if Prx1 gets stabilized after the treatment, because it has an irreversible inhibitory effect on proteasome. HEK293T cells were transfected with pCAG-FLAG-Prx1 plus either empty vector or pCAG-HA-E6AP. Overexpression of E6AP resulted in a remarkable reduction of the Prx1 (Fig. 4D, lane 2, middle panel), whereas the Prx1 protein level was increased after treatment with clasto-lactacystin (Fig. 4D, lane 4, middle panel). In contrast, the Prx1 protein level was unchanged after treatment with E-64d plus Pepstatin A (Fig. 4D, lane 6, middle panel). These results indicate that E6AP-induced reduction of Prx1 is proteasome-dependent.

E6AP-DEPENDENT POLYUBIQUITYLATION OF Prx1 IN VIVO

To determine whether E6AP can induce ubiquitylation of Prx1 in cells, we performed in vivo ubiquitylation assays. HEK293T cells were transfected with FLAG-Prx1 plasmid and either E6AP or Nedd4 plasmid, together with a plasmid encoding HA-tagged ubiquitin to facilitate the detection of ubiquitylated Prx1. Cell lysates were immunoprecipitated with anti-FLAG MAb and immunoblotted with anti-HA PAb to detect ubiquitylated Prx1 protein. No ubiquitin signal was detected in the cells co-transfected with empty plasmid or Nedd4 plasmid (Fig. 5A, lanes 4 and 6). In contrast, co-expression of E6AP led to readily detectable polyubiquitylated forms of the Prx1 as a smear of higher-molecular weight bands (Fig. 5A, left panel, lane 5). Immunoblot analysis with anti-FLAG PAb confirmed that FLAG-Prx1 was immunoprecipitated and that higher-molecular weight bands conjugated with HA-ubiquitin were indeed poly-ubiquitylated forms of the FLAG-Prx1 (Fig. 5A, right panel, lane 5). These results suggest that E6AP enhances polyubiquitylation of Prx1 in vivo.

To further investigate if E6AP is involved in K48-linked ubiquitylation of Prx1, we performed in vivo ubiquitylation assay using HA-tagged K48R dominant negative ubiquitin mutant and K48 only ubiquitin mutant expression plasmids. HEK293T cells were transfected with FLAG-Prx1 plasmid and E6AP plasmid, together with a plasmid encoding HA-ubiquitin WT, HA-K48R ubiquitin, or HA-K48 ubiquitin to facilitate the detection of ubiquitylated Prx1. Ubiquitin signal was detected in the cells transfected with either HA-ubiquitin WT or HA-K48 ubiquitin plasmid (Fig. 5B, lane 1 or 3), whereas no ubiquitin signal was detected in the cells transfected with HA-K48R ubiquitin (Fig. 5B, lane 2), suggesting that E6AP enhances K48-linked polyubiquitylation of Prx1. These results are consistent with the notion that E6AP is involved in proteasomal degradation of Prx1.

E6AP MEDIATES POLYUBIQUITYLATION OF Prx1 IN VITRO

To reconstitute the E6AP-mediated polyubiquitylation of Prx1 in vitro, we performed an in vitro ubiquitylation assay of the Prx1 using purified MEF-E6AP and His_6-Prx1 as described above. When the in vitro ubiquitylation reaction was carried out in the presence of MEF-E6AP C-A, no ubiquitylation signal was detected (Fig. 5C, lanes 3). However, inclusion of purified MEF-E6AP in the reaction mixture resulted in ubiquitylation of His_6-Prx1 (Fig. 5C, lane 4). No signal was detected when His_6-Prx1 was not included in the reaction mixture (Fig. 5C, lane 2). From these results, we concluded that E6AP mediates polyubiquitylation of Prx1.

DISCUSSION

In this study, we identified Prx1 as a novel E6AP-binding protein using a tandem affinity purification procedure coupled with mass spectrometry. Overexpression of E6AP enhances proteasomal degradation of Prx1, and siRNA-mediated knockdown of endogenous E6AP results in accumulation of endogenous Prx1. E6AP enhances the polyubiquitylation of Prx1 in vivo and in vitro. We conclude that E6AP mediates ubiquitin-dependent degradation of

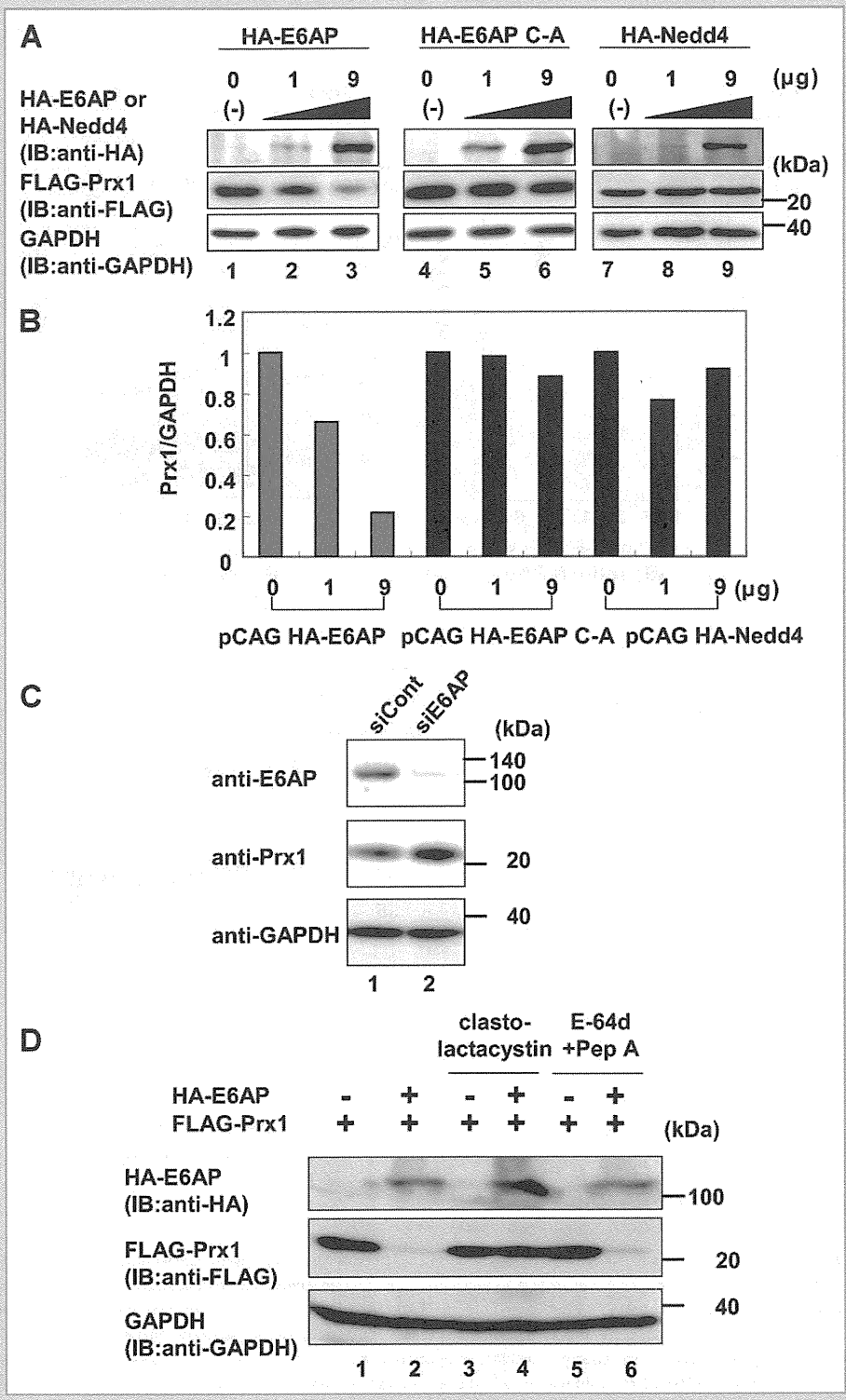

Fig. 4. E6AP decreases the steady-state levels of Prx1 protein in HEK293T cells. A: HEK293T cells (5×10^5 cells/six-well plate) were transfected with 0.5 μg pCAG-FLAG-Prx1 plus empty vector and 1 or 9 μg of pCAG-HA-E6AP, pCAG-HA-E6AP C-A, or pCAG-HA-Nedd4. At 48 h posttransfection, equivalent amounts of the whole-cell lysates were separated by SDS-PAGE and analyzed by immunoblotting with anti-HA MAb (top panel), anti-FLAG MAb (middle panel), and anti-GAPDH MAb (bottom panel). The results shown are representative of three independent experiments. B: Quantitation of the data shown in panel A. The intensities of the gel bands were quantitated using the ImageJ 1.43 program. The level of GAPDH served as a loading control. C: Knockdown of endogenous E6AP by siRNA resulted in the accumulation of endogenous Prx1 in HEK293T cells. HEK293T cells (3×10^5 cells/six-well plate) were transfected with 40 pmol of E6AP-specific duplex siRNA (or a scramble negative control). The cells were harvested at 96 h after siRNA transfection. D: HEK293T cells (5×10^5 cells/six-well plate) were transfected with 0.5 μg of pCAG-FLAG-Prx1 plus 9 μg of empty vector or pCAG-HA-E6AP. At 36 h after transfection, the cells were treated with DMSO control (lanes 1 and 2), 30 μM clasto-lactacystin (lanes 3 and 4), or 40 μM E-64d plus 20 μM Pepstatin A (lanes 5 and 6). Cells were collected at 12 h after treatment with the inhibitors. Equivalent amounts of the whole-cell lysates were separated by SDS-PAGE and analyzed by immunoblotting with anti-HA MAb (upper panel), anti-FLAG MAb (middle panel), or anti-GAPDH MAb (lower panel).

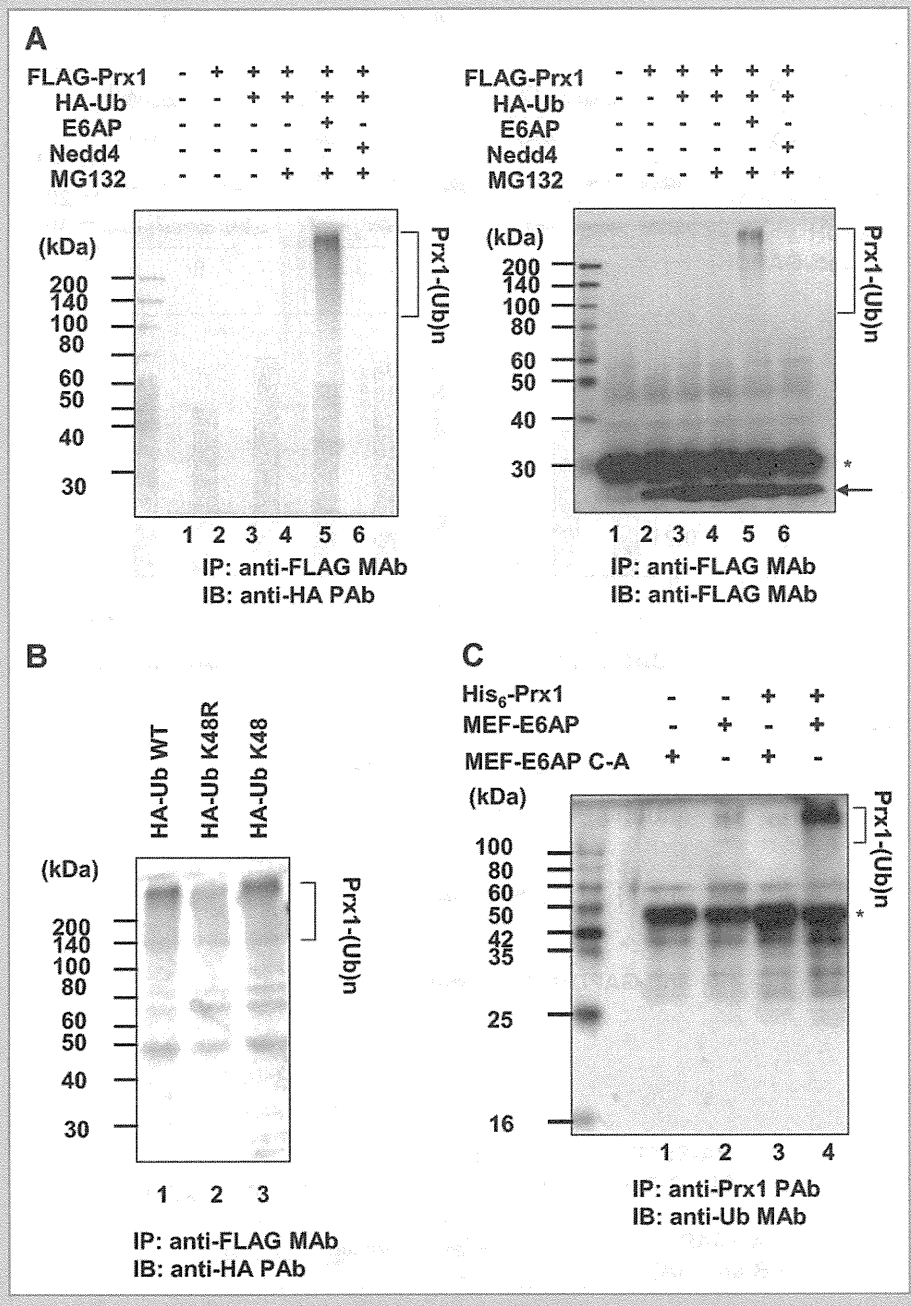

Fig. 5. E6AP mediates ubiquitylation of Prx1 in vivo and in vitro. A: HEK293T cells (2×10^6 cells/10-cm dish) were transfected with 1 μg of pCAG-FLAG-Prx1 together with 2 μg of plasmid encoding E6AP or Nedd4 as indicated. Each transfection also included 2 μg of plasmid encoding HA-ubiquitin. The cell lysates were immunoprecipitated with FLAG beads and analyzed by immunoblotting with anti-HA PAb (left panel) or anti-FLAG MAb (right panel). Arrow indicates FLAG-Prx1. Asterisk indicates immunoglobulin light chain. Ubiquitylated species of FLAG-Prx1 are marked by brackets. B: HEK293T cells (2×10^6 cells/10-cm dish) were transfected with 1 μg of pCAG-FLAG-Prx1 together with 2 μg of plasmid encoding E6AP plasmid. Each transfection also included 2 μg of plasmid encoding HA-Ub WT, HA-Ub K48R, or HA-Ub K48 as indicated. At 36 h after transfection, the cells were treated with 25 μM MG132 and cultured for 12 h. The cell lysates were immunoprecipitated with FLAG beads and analyzed by immunoblotting with anti-HA PAb. Ubiquitylated species of FLAG-Prx1 are marked by brackets. C: In vitro ubiquitylation of Prx1 by recombinant E6AP. For in vitro ubiquitylation of Prx1 protein, purified His_6-Prx1 was used as a substrate. Assays were done in 40-μl volumes containing each component as indicated. The reaction mixture is described in Materials and Methods Section. The reaction was carried out at 37°C for 120 min followed by immunoprecipitation with anti-Prx1 PAb and analysis by immunoblotting with anti-Ub MAb. Ubiquitylated species of His_6-Prx1 are marked by brackets. Asterisk indicates immunoglobulin heavy chain.

Prx1. Our results suggest that E6AP is involved in the regulation of Prx1 activity through the ubiquitin–proteasome pathway.

Prx1 is a 25-kDa member of the Prx family, a ubiquitous family of antioxidant peroxidases that regulate many cellular processes through intracellular oxidative signal transduction pathways. More than 50 members of the Prx family have been identified in a wide variety of organisms ranging from prokaryotes to mammals. Prxs are widely expressed hydrogen peroxide scavenger proteins best